Kinetic Mechanism of DNA Binding and DNA-Induced Dimerization of the *Escherichia coli* Rep Helicase†

Keith P. Bjornson, Keith J. M. Moore, and Timothy M. Lohman*

Department of Biochemistry and Molecular Biophysics, Box 8231, Washington University School of Medicine, 660 S. Euclid Avenue, St. Louis, Missouri 63110

Received September 22, 1995; Revised Manuscript Received December 4, 1995⊗

ABSTRACT: The monomeric *Escherichia coli* Rep protein undergoes a DNA-induced dimerization upon binding either single-stranded (ss) or duplex DNA with the dimer being the active form of the Rep helicase. Using stopped-flow fluorescence, we have determined a minimal kinetic mechanism for this reaction in which Rep monomer (P) binds to ss oligodeoxynucleotides ($dN(pN)_{15}$) (S) by a two-step mechanism to form PS*, which can then dimerize with P to form P_2S as indicated: $2P + S \underset{k_{-1}}{\overset{k_1}{\rightleftharpoons}} PS + P \underset{k_{-2}}{\overset{k_2}{\rightleftharpoons}} PS^* + P \underset{k_{-3}}{\overset{k_3}{\rightleftharpoons}} P_2S$. This minimal mechanism is supported by four independent studies in which the kinetics were monitored by changes in fluorescence intensity of three different probes: the intrinsic Rep tryptophan fluorescence, the fluorescence of $d(T_5(2\text{-AP})T_4(2\text{-AP})T_5)$, containing the fluorescent base, 2-aminopurine (2-AP), and $dT(pT)_{15}$ labeled at its 3′-end with fluorescein (3′-F-$dT(pT)_{15}$). Simultaneous (global) analysis of the time courses of $d(T_5(2\text{-AP})T_4(2\text{-AP})T_5)$ (100 nM) binding to a range of Rep monomer concentrations (25−400 nM) yields the following rate constants: $k_1 = (3.3 \pm 0.5) \times 10^7$ M^{-1} s^{-1}; $k_{-1} = 1.4 \pm 0.4$ s^{-1}; $k_2 = 2.7 \pm 0.9$ s^{-1}; $k_{-2} = 0.21 \pm 0.06$ s^{-1}; $k_3 = (4.5 \pm 0.3) \times 10^5$ M^{-1} s^{-1}; $k_{-3} = 0.0027 \pm 0.0008$ s^{-1} [20 mM Tris-HCl, pH 7.5, 6 mM NaCl, 5 mM $MgCl_2$, 5 mM 2-mercaptoethanol, and 10% (v/v) glycerol, 4.0 °C]. This mechanism provides direct evidence that Rep monomers can bind ss DNA and that ss DNA binding induces a conformational change in the Rep monomer that is probably required for Rep dimerization. This conformational change is likely to be large and global since it is detected by all three fluorescence probes. The apparent bimolecular rate constant for Rep monomer binding to 3′-F-$dT(pT)_{15}$ [k_1(app) $= (6.0 \pm 0.7) \times 10^7$ M^{-1} s^{-1}] is slightly larger than measured with $d(T_5(2\text{-AP})T_4(2\text{-AP})T_5)$ binding. The apparent rate constant for dissociation of $d(T_5(2\text{-AP})T_4(2\text{-AP})T_5)$ (S) from the half-ligated Rep dimer, P_2S, increases with increasing concentration of a nonfluorescent competitor ss DNA ($d(T_5AT_4AT_5)$) (C), indicating transient formation of a doubly ligated P_2SC intermediate. However, the apparent bimolecular rate constant for binding of C to P_2S is extremely slow (≥ 250 M^{-1} s^{-1}), suggesting the occurrence of a multistep process before dissociation of ss DNA. In the absence of competitor DNA, dissociation of ss DNA from P_2S occurs only after slow dissociation of the Rep dimer to form PS* + P. The implications of these results for Rep-catalyzed DNA unwinding are discussed.

DNA helicases are a class of motor proteins that catalyze the unwinding of duplex DNA by utilizing the energy obtained from binding and hydrolysis of nucleoside triphosphates to destabilize the base pairs between complementary DNA strands and to translocate along the DNA (Matson & Kaiser-Rogers, 1990; Lohman, 1992, 1993; Lohman & Bjornson, 1996). These enzymes appear to be ubiquitous, having been identified in prokaryotes, eukaryotes, bacteriophages, and viruses, and function in all aspects of DNA metabolism, including DNA replication, repair, and recombination (Matson et al., 1994); DNA helicases also function in the coupling of DNA repair and transcription (Hanawalt, 1994). Whereas many helicases have been characterized biochemically, studies of their mechanisms of DNA unwinding and translocation are in their early stages. Although it is clear that no single mechanism for DNA unwinding is used by all DNA helicases, a few general features seem to characterize these enzymes. In particular, all DNA helicases for which the assembly state has been characterized carefully appear to form oligomers, generally dimers or hexamers (Lohman, 1992, 1993; Lohman & Bjornson, 1996). The oligomeric nature of DNA helicases provides the active helicase with multiple DNA and nucleoside triphosphate binding sites that seem to be necessary for DNA unwinding activity.

The *Escherichia coli* Rep helicase, one of the first DNA helicases to be discovered and characterized biochemically (Lane & Denhardt, 1974, 1975; Scott et al., 1977; Yarranton & Gefter, 1979; Kornberg et al., 1978; Arai & Kornberg, 1981; Arai et al., 1981), is one of a few DNA helicases that has been studied at a mechanistic level. Although all of its physiological roles have not yet been established, the Rep helicase is involved in DNA replication (Lane & Denhardt, 1974, 1975; Colasanti & Denhardt, 1987), has been implicated in DNA repair and recombination (Calendar et al.,

† This work was supported in part by grants to T.M.L. from the NIH (GM 45948) and the American Cancer Society (NP-756B). K.P.B. received partial support from an NIH Training Grant (5 T32 GM08492), and K.J.M.M. received partial support from a William M. Keck Foundation Fellowship.

* Tel: (314) 362-4393. FAX: (314) 362-7183.

⊗ Abstract published in *Advance ACS Abstracts,* January 15, 1996.

0006-2960/96/0435-2268$12.00/0

1970; Bridges & von Wright, 1981), and is essential for replication of several bacteriophages, including ϕX174 (Denhardt et al., 1967). The *E. coli rep* gene encodes a single polypeptide (673 amino acids, M_r 76 400) which exists as a monomer in the absence of DNA at concentrations up to its solubility limit (Chao & Lohman, 1991). However, binding of either ss or duplex DNA induces Rep to dimerize with high affinity [dimerization constant, $L_{2S} = (1-2) \times 10^8$ M^{-1} at 4 °C] (Wong et al., 1992; Wong & Lohman, 1992), and the dimer appears to be the active form of the Rep helicase (Chao & Lohman, 1991; Amaratunga & Lohman, 1993; Bjornson et al., 1994). Each subunit of the Rep dimer contains both a nucleotide binding site (Moore & Lohman, 1994a,b) and a DNA binding site (Wong et al., 1992). Both subunits of the Rep dimer can bind either ss or double-stranded (ds) DNA competitively; however, the Rep dimer can also bind both ss and ds DNA simultaneously, with one DNA conformation bound to each subunit (Wong et al., 1992). Furthermore, the DNA binding sites within the dimer exhibit negative cooperativity such that the affinity of DNA to the second site (subunit) of the dimer is significantly weaker than to the first site (Wong et al., 1992; Wong & Lohman, 1992). The affinity of DNA (either ss or ds) for the second subunit is also influenced by the conformation of DNA that occupies the first subunit. Of most interest is the observation that the relative affinity of the second site for DNA is modulated allosterically by nucleotide binding (ATP, ADP, or AMPPNP) (Wong & Lohman, 1992).

These observations led to the proposal of an "active, rolling" mechanism for DNA unwinding by the dimeric Rep helicase (Wong & Lohman, 1992), which has been further supported by kinetic studies of DNA unwinding (Amaratunga & Lohman, 1993; Bjornson et al., 1994). In each step of this mechanism, at least one subunit of the Rep dimer (although not always the same subunit) remains bound to ss DNA while the other subunit is unligated, bound to ss DNA, or bound to duplex DNA. Translocation of Rep is proposed to be coupled to ATP binding and to occur by a rolling mechanism in which one subunit dissociates from ss DNA and rebinds to the duplex region ahead of the fork while the other subunit remains bound to ss DNA. DNA unwinding is proposed to be coupled to ATP hydrolysis and to occur by "melting" a region of duplex DNA to which one subunit of the Rep dimer was bound (Wong & Lohman, 1992).

This active, rolling model was proposed based on equilibrium studies of Rep−DNA binding (Wong & Lohman, 1992). However, a molecular understanding of the mechanism by which the dimeric Rep helicase unwinds duplex DNA requires kinetic information for each step of the mechanism. This in turn requires investigations of the kinetic mechanism of DNA binding (both ss and ds DNA to Rep monomer and both subunits) and DNA-induced Rep dimerization. Finally, one must determine how each step in the unwinding mechanism is coupled to ATP binding and hydrolysis. Toward this goal, studies of the mechanism of nucleotide binding to Rep monomers (Moore & Lohman, 1994a,b) and Rep dimers (Moore & Lohman, 1995) have been initiated.

In this report, we have used stopped-flow fluorescence techniques to examine the kinetics and mechanism of Rep monomer binding to ss oligodeoxynucleotides and the subsequent DNA-induced Rep dimerization by monitoring fluorescence probes in both the protein and the DNA. As in our previous equilibrium binding studies (Chao & Lohman, 1991; Wong et al., 1992; Wong & Lohman, 1992), we use ss oligodeoxynucleotides ($dN(pN)_{15}$) that are short enough so that only one Rep monomer or dimer subunit can bind per DNA which facilitates resolution of the kinetics of DNA binding from DNA-induced Rep dimerization. We have examined a wide range of protein and DNA concentrations spanning both excess DNA and excess Rep protein and have determined the rate constants for a minimal mechanism which is consistent with all of the fluorescence probes examined.

MATERIALS AND METHODS

Buffers and Rep Protein. Buffers were made with reagent grade chemicals using glass distilled H_2O that was deionized using a Milli-Q System (Millipore Corp., Bedford, MA). Buffer A is 20 mM Tris-HCl titrated to pH 7.5 at 4.0 °C, 6 mM NaCl, 5 mM $MgCl_2$, 5 mM 2-mercaptoethanol, and 10% (v/v) glycerol (spectrophotometric grade, Fisher, Fair Lawn, NJ). *E. coli* Rep protein was purified to >99% homogeneity as described (Lohman et al., 1989), and its concentration was determined spectrophotometrically, based on the extinction coefficient for the monomer of $\epsilon_{280} = 7.68 \times 10^4$ M^{-1} cm^{-1} (Amaratunga & Lohman, 1993).

Preparation of DNA Substrates. All oligodeoxynucleotides used in these studies were hexadecamers ($dN(pN)_{15}$) and were synthesized using an ABI model 391 automated DNA synthesizer (Applied Biosystems, Foster City, CA) with standard β-cyanoethyl phosphoramidite chemistry. Phosphoramidites, including 2-aminopurine (2-AP) were purchased from Glenn Research (Sterling, VA). The sequence of the oligodeoxynucleotide containing 2-AP is 5′-d(TTTTT-(2-AP)TTTT(2-AP)TTTTT). The $dT(pT)_{15}$ with fluorescein (F) attached to its 3′ end via a six-carbon linker was prepared using a fluorescein-CPG column support (Glenn Research, Sterling, VA) as described (Bjornson et al., 1994). Oligodeoxynucleotides were deblocked and purified to >99% homogeneity by polyacrylamide gel electrophoresis (PAGE) as described (Amaratunga & Lohman, 1993). The oligodeoxynucleotide concentrations were determined by absorbance at 260 nm using extinction coefficients of 115 400 M^{-1} cm^{-1} for $d(T_5(2\text{-AP})T_4(2\text{-AP})T_5)$, 129 600 M^{-1} cm^{-1} for $dT(pT)_{15}$, and 131 240 M^{-1} cm^{-1} for 3′-F-$dT(pT)_{15}$ [accounting for the contribution of fluorescein absorbance at 260 nm (Bjornson et al., 1994)].

Fluorescence Stopped-Flow Kinetics. Stopped-flow fluorescence experiments were carried out using either an Applied Photophysics SX17MV stopped-flow (Applied Photophysics Ltd., Leatherhead, U.K.) supplied with a 150 W Xe arc lamp or a KinTek SF-2001 stopped-flow (KinTek, Inc., University Park, PA) equipped with a 75 W Xe lamp. Rep tryptophan fluorescence ($\lambda_{ex} = 290$ nm) was monitored at wavelengths >320 nm using a cut-on filter (Oriel Corp., Stratford CT, catalog no. 51255). Fluorescein fluorescence ($\lambda_{ex} = 492$ nm) was monitored at wavelengths >520 nm using a cut-on filter (Oriel catalog no. 51300). 2-Aminopurine fluorescence ($\lambda_{ex} = 310$ or 315 nm as indicated) was monitored at wavelengths >350 nm using a cut-on filter (Oriel catalog no. 51260). A wavelength of 315 nm was used to excite 2-AP fluorescence instead of the excitation maximum at 310 nm (Ward et al., 1969) when it was necessary to avoid simultaneous excitation of tryptophan fluorescence. All slit widths were 1−2 mm. All concentrations reported

are the final concentrations of reactants in the flow cell after mixing. The kinetic traces shown generally represent an average of 3−16 individual determinations, and the indicated errors in the fitted parameters represent the standard error. Reactants were stored on ice and then incubated for at least 5 min in the stopped-flow prior to mixing in order to thermally equilibrate the samples at 4.0 °C. When applicable, the fluorescence time courses were fit to single or sums of exponential terms as in eq 1

$$F(t) = \sum A_n[1 - \exp(-k_{\mathrm{obs},n}t)] + F(0) \qquad (1)$$

where $F(t)$ is the fluorescence at time t, n is the number of exponential terms, A_n and $k_{\mathrm{obs},n}$ are the amplitude and the observed rate constant for the nth term, respectively, and $F(0)$ is the fluorescence intensity at time zero. The overall fluorescence enhancement, E, for the 2-aminopurine experiments in Figure 2 was calculated using eq 2

$$E = (A/F_{\mathrm{DNA}})([\mathrm{DNA}]_{\mathrm{total}}/[\mathrm{Rep}]_{\mathrm{total}}) + 1 \qquad (2)$$

where A is the pre-exponential amplitude determined from the fit to a single-exponential time course and F_{DNA} is the fluorescence of the free oligodeoxynucleotide determined at each DNA concentration.

Equilibrium Fluorescence Titrations. Equilibrium fluorescence titrations of the 2-AP containing oligodeoxynucleotide, $d(T_5(2\text{-AP})T_4(2\text{-AP})T_5)$, with Rep were performed using an SLM 8000 spectrofluorimeter (SLM-Aminco, Urbana, IL) in buffer A at 4 °C. The excitation wavelength was 310 or 315 nm as indicated (2 mm slits), and emission fluorescence was monitored at wavelengths >350 nm using a cut-on filter (2 in. diameter; Oriel catalog no. 59460). For each titration of DNA with Rep, we also performed a blank titration of buffer A with Rep. For each point "*i*" in the titration, the corrected fluorescence, F_i, was obtained as $F_i = f_{\mathrm{obs},i} - f_{\mathrm{blank},i}$, where $f_{\mathrm{blank},i}$ and $f_{\mathrm{obs},i}$ are the fluorescence intensities for point "*i*" determined in the blank titration and the actual titration, respectively. The fraction of maximal fluorescence enhancement was calculated as $(F_i - F_o)/(F_{\max} - F_o)$, where F_o is the initial fluorescence of the DNA sample before addition of Rep. After each addition of Rep protein, the sample was stirred with a polyethylene rod and equilibrated for at least 10 min with the shutters closed.

Steady State Kinetics of ATP Hydrolysis. Stock solutions of ATP were prepared as described (Moore & Lohman, 1994a,b). The steady state kinetics of ATP hydrolysis by Rep protein in the presence of $dT(pT)_{15}$ were measured in buffer A at 4.0 °C and are reported as initial velocities (μM ATP hydrolyzed s^{-1}). Reactions were initiated by mixing a pre-equilibrated Rep−DNA solution (2.0 μM $dT(pT)_{15}$ and 0.1−2.0 μM Rep) with an equal volume of 2 mM ATP containing [α-^{32}P]ATP (Amersham, Arlington Heights, IL) (final specific activity, ~20 mCi/mol of ATP). Aliquots (20 μL) were removed at defined time intervals and quenched by the addition of an equal volume of 0.5 M Na_3EDTA pH 8.0. The [α-^{32}P]ADP product was resolved from [α-^{32}P]-ATP by thin-layer chromatography (TLC) on PEI-cellulose (E. Merk, Darmstadt, Germany) using 0.3 M potassium phosphate (pH 7.0) as the mobile phase (Patel et al., 1991). Quantitation of the radiolabeled ATP and ADP was performed by imaging the TLC plates using a Betascope 603 blot analyzer (Betagen, Waltham, MA).

The ATPase activity of Rep was determined in the presence of $dT(pT)_{15}$ (1 μM) as a function of total [Rep]. These were compared to predicted ATPase activity based on the population distribution of Rep monomer (PS + PS*) and dimer species (P_2S and P_2S_2) calculated from the equilibrium constants (K_1, K_2, and K_3) that were determined from the kinetic measurements reported here (Table 1) and the known k_{cat} values for these Rep species. These were also compared to the predicted ATPase activity based on the equilibrium population distributions for PS, P_2S, and P_2S_2 calculated from the equilibrium constants determined previously by nitrocellulose filter binding (Wong et al., 1992; Wong & Lohman, 1992). The values of k_{cat} for each Rep species were determined independently from experiments performed under the conditions of these experiments (buffer A, 4 °C) at protein and DNA concentrations that optimize the population of each individual species (K. J. M. Moore, unpublished). The value of $k_{\mathrm{cat,(PS + PS^*)}} = 2 \pm 0.5\ s^{-1}$ was determined under conditions that populated only the Rep monomer species (PS + PS*) (i.e., low Rep concentrations and $[dT(pT)_{15}] \gg [\mathrm{Rep}]$). The value of $k_{\mathrm{cat,P_2S}} = 18 \pm 2\ s^{-1}$ was determined under conditions of $[\mathrm{Rep}] \gg [dT(pT)_{15}]$. The value of $k_{\mathrm{cat,P_2S_2}} = 68 \pm 2\ s^{-1}$ was determined from studies of cross-linked Rep−$dT(pT)_{15}$ complexes (I. Wong and T. M. Lohman, manuscript in preparation).[1] A value of $k_{\mathrm{cat,P}} = 0.002\ s^{-1}$ was determined previously for the unligated Rep monomer (Moore & Lohman, 1994a), and thus ATP hydrolysis by this species is negligible compared to the DNA-ligated Rep species. The initial velocity for ATP hydrolysis, $V_{\mathrm{o,obs}}$ (μM ATP hydrolyzed s^{-1}) was calculated using eq 3.

$$V_{\mathrm{o,obs}} = 2([\mathrm{PS}] + [\mathrm{PS^*}]) + 18[\mathrm{P_2S}] + 68[\mathrm{P_2S_2}] \qquad (3)$$

The concentrations of each Rep species were calculated for each total Rep concentration at constant total $[dT(pT)_{15}]$ as described by Wong et al. (1992) using Scheme 5 and the equilibrium constants reported in Table 1[1] or Scheme 1 and the equilibrium constants (K_{1S}, L_{2S}, K_{2SS}) determined previously in the absence of nucleotides (Wong & Lohman, 1992).

Analysis of Kinetic Data. The kinetic traces were analyzed using the software provided by the manufacturer of each stopped-flow instrument (version 4.099 run on an Archimedies work-station for Applied Photophysics and version 3.0 run on a Swan 486 PC for KinTek). Simulations and plots were constructed and analyzed using the program KaleidaGraph (Synergy Software, Reading PA) run on a Macintosh II computer. The global numerical analysis of kinetic time courses was performed using PC versions of KINSIM and FITSIM (Barshop et al., 1983; Zimmerle & Frieden, 1989)

[1] Our current estimates of K_4 (K_{2SS}) and k_{cat} for the fully saturated P_2S_2 dimer are $K_{2SS} = 0.07\ \mu M^{-1}$ and $k_{\mathrm{cat}} = 68\ s^{-1}$. This value of K_4 (K_{2SS}) is greater than that determined under these same conditions by filter binding ($0.009 \pm 0.001\ \mu M^{-1}$) (Wong & Lohman, 1992). However, even with this higher estimate of K_{2SS}, the population of P_2S_2 dimers is very low under the experimental conditions used in these studies, as shown in Figure 9. Furthermore, our ability to differentiate between the two sets of equilibrium constants on the basis of the results in Figure 9 is independent of these constants since the different qualitative dependences of Rep ATPase activity on [Rep] are sensitive only to the relative populations of PS and P_2S. The equilibrium constants in Table 1 predict a nonlinear dependence of ATPase activity on [Rep] (mirroring P_2S formation), whereas the equilibrium constants determined from our previous filter binding measurements (Wong & Lohman, 1992) predict a linear dependence. The curves in Figure 9 were simulated using a k_{cat} value of $68\ s^{-1}$ for ATP hydrolysis by P_2S_2 and a K_{2SS} value of $0.07\ \mu M^{-1}$. (Wong et al., submitted).

Scheme 1

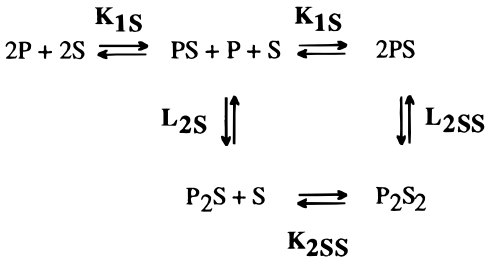

(kindly provided by Dr. Carl Frieden of this department) and were run on an IBM PS/2 76 computer.

RESULTS

Previous equilibrium studies of ss DNA binding to *E. coli* Rep monomer (Wong et al., 1992; Wong & Lohman,1992) are consistent with Scheme 1, and the equilibrium constants for ss DNA binding (K_{1S}, K_{2SS}) and Rep dimerization (L_{2SS}, L_{2S}) were determined using ss oligodeoxynucleotides that are short enough ($dN(pN)_{15}$) to ensure that only one ss oligodeoxynucleotide can bind per Rep monomer or to each subunit of a Rep dimer. These and other studies (Chao & Lohman, 1991) indicate that Rep dimers do not form in the absence of DNA binding up to concentrations of at least 10 μM; however, Rep monomers (P) can bind DNA (S) to form PS, which can then dimerize with either P or PS to form the half-ligated dimer, P_2S, or the fully ligated dimer, P_2S_2. The studies described below were designed to determine the elementary rate constants for the steps in Scheme 1 and to probe for the presence of additional intermediates.

Kinetics of Rep Monomer Binding to Excess ss DNA Monitored by Rep Tryptophan Fluorescence Quenching. Rep protein contains eight tryptophans per monomer on the basis of its amino acid sequence as predicted from the revised DNA sequence of the *rep* gene (Daniels et al., 1992), and the Rep monomer displays a typical fluorescence emission spectrum with maximum emission wavelength at 343 nm (λ_{ex} = 290 nm) (data not shown). Furthermore, upon saturation of Rep with the oligodeoxynucleotide, $dT(pT)_{15}$, the Trp fluorescence intensity is quenched by ~20%. We therefore performed stopped-flow kinetics of Rep binding to single-stranded (ss) oligodeoxynucleotides ($dN(pN)_{15}$) by monitoring the quenching of Rep Trp fluorescence.

Our initial experiments were designed to examine the kinetics of $dN(pN)_{15}$ binding to Rep monomer in the absence of Rep dimerization. Recall that Rep protein is monomeric and dimerization is induced only upon binding DNA (Chao & Lohman, 1991; Wong & Lohman, 1992; Wong et al., 1992). Furthermore, under the conditions of our experiments (buffer A, 4 °C), the dimerization constant to form the fully ligated P_2S_2 dimer ($L_{2SS} \approx 9 \times 10^5$ M^{-1}) is ~200-fold smaller than the dimerization constant to form the half-ligated P_2S dimer [$L_{2S} = (2 \pm 0.4) \times 10^8$ M^{-1}] (Wong & Lohman, 1992). Therefore, the experiments described in Figures 1 and 2 were performed at sufficiently low Rep concentrations and excess ss DNA such that the population of Rep dimers is negligible at equilibrium. A series of stopped-flow kinetics experiments were performed in buffer A at 4.0 °C by mixing Rep (100 nM total monomer concentration) with $d(T_4AT_5AT_4)$ at concentrations ranging from 0.1 to 5.0 μM. This DNA sequence was used in order to better compare these experiments with those (see below) that were performed with

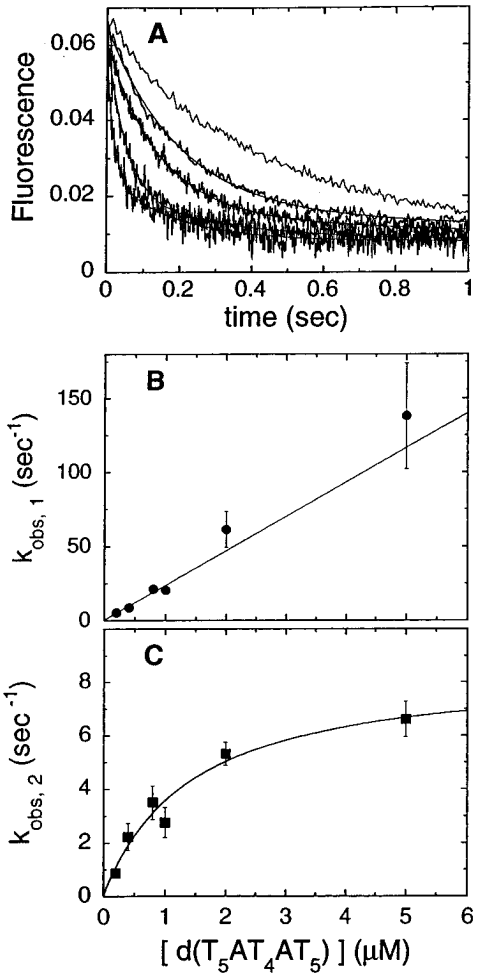

FIGURE 1: Kinetics of Rep monomer binding to an excess of the ss oligodeoxynucleotide, $d(T_5AT_4AT_5)$, monitored by quenching of the intrinsic tryptophan fluorescence (arbitrary units) of the Rep protein. A. Stopped-flow kinetic traces monitoring Rep Trp fluorescence (λ_{ex} = 290 nm, λ_{em} > 320 nm) upon mixing 100 nM Rep monomer (final concentration) with 0.1 (top trace), 0.2, 0.4, 0.8, and 2.0 μM (bottom trace) $d(T_5AT_4AT_5)$ in buffer A at 4.0 °C. The solid lines overlaying each time course are nonlinear least-squares fits of the data to the sum of two exponential decays, with observed rate constants $k_{obs,1}$ and $k_{obs,2}$. B. Observed rate constant of the fast phase, $k_{obs,1}$ (●), obtained from the fits shown in panel A, plotted as a function of [DNA]. The linear least-squares fits to the data (solid line) has a slope of $(2.3 \pm 0.2) \times 10^7$ M^{-1} s^{-1} and an intercept of 0.5 ± 0.4 s^{-1}. C. Observed rate constant for the second phase, $k_{obs,2}$ (■), obtained from the fits shown in panel A, plotted as a function of [DNA]. The solid curve is a nonlinear least-squares fits of the data to a hyperbola with a zero intercept, an apparent $K_d = 1.4 \pm 0.4$ μM, and a plateau of 8.5 ± 1.0 s^{-1}.

$d(T_5(2\text{-AP})T_4(2\text{-AP})T_5)$ containing the fluorescent base analogue 2-aminopurine (2-AP). However, identical results were obtained with $dT(pT)_{15}$ (data not shown). Figure 1A shows kinetic time courses for experiments performed at 0.1, 0.2, 0.4, 0.8, and 2.0 μM $d(T_4AT_5AT_4)$. In each experiment a biphasic time course for the quenching of Rep Trp fluorescence is observed which is well described by the sum of two exponentials (see eq 1). If Rep monomer binding to $d(T_4AT_5AT_4)$ occurs by a simple one-step mechanism, then a single-exponential time course would be observed under conditions that are pseudo first order in DNA (Johnson, 1992). This indicates that Rep monomer binding to $d(T_4AT_5AT_4)$ occurs by a mechanism with a minimum of two steps. The observation that biphasic kinetics persists even at a 50-fold excess of ss DNA over Rep monomer where all Rep monomer is bound to DNA (bottom trace in Figure 1A),

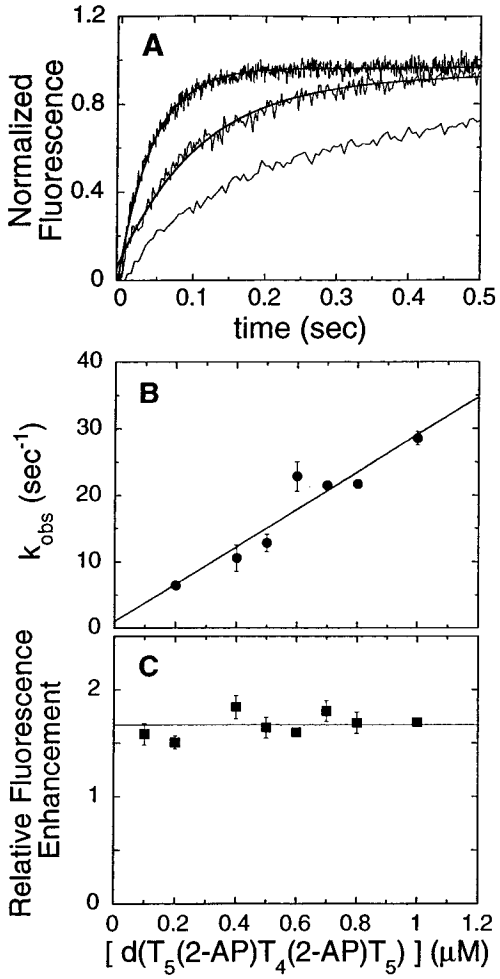

FIGURE 2: Kinetics of Rep monomer binding to an excess of the fluorescent ss oligodeoxynucleotide, d(T_5(2-AP)T_4(2-AP)T_5), as monitored by the enhancement of the 2-aminopurine (2-AP) fluorescence. A. Stopped-flow kinetic traces monitoring DNA (2-AP) fluorescence (λ_{ex} = 315 nm, λ_{em} > 350 nm) upon mixing 100 nM Rep monomer (final concentration) with 0.7 (top trace), 0.2, 0.1 μM (bottom trace) d(T_5(2-AP)T_4(2-AP)T_5) in buffer A at 4.0 °C. The nonlinear least-squares fits to a single-exponential curve with observed rate constant, k_{obs}, are shown for the experiments at 0.7 and 0.2 μM d(T_5(2-AP)T_4(2-AP)T_5), which are conditions of excess oligodeoxynucleotide. The total amplitude of each time course was normalized to the maximum observed fluorescence enhancement. B. The dependence on total [d(T_5(2-AP)T_4(2-AP)-T_5)] of the observed rate constant, k_{obs} (●), obtained from a single-exponential fit of each fluorescence time courses. The solid line is the linear least-squares fits to the data, with slope and intercept of $(2.8 \pm 0.7) \times 10^7$ M^{-1} s^{-1} and 0.9 ± 0.4 s^{-1}, respectively. C. The relative enhancement of 2-AP fluorescence (■) is independent of the total d(T_5(2-AP)T_4(2-AP)T_5) concentration. The solid line represents the average value of 1.7 ± 0.1.

Scheme 2

$$P + S \underset{k_{-1}}{\overset{k_1}{\rightleftharpoons}} PS \underset{k_{-2}}{\overset{k_2}{\rightleftharpoons}} PS^*$$

indicates that the second step is accompanied by additional tryptophan fluorescence quenching.

The mechanism in Scheme 2, in which the binding step is followed by an isomerization, predicts a biphasic kinetic time course. Under pseudo-first-order conditions, the observed rate constants for the fast phase, $k_{obs,1}$, and the slower phase, $k_{obs,2}$, can be approximated by eqs 4 and 5, respectively (Johnson, 1992).

$$k_{obs,1} \approx k_1[\text{DNA}] + k_2 + k_{-2} + k_{-1} \quad (4)$$

$$k_{obs,2} \approx \frac{k_1[\text{DNA}](k_2 + k_{-2}) + k_{-1}k_{-2}}{k_1[\text{DNA}] + k_2 + k_{-2} + k_{-1}} \quad (5)$$

The experimental values of $k_{obs,1}$ and $k_{obs,2}$, obtained by fitting the time courses to a double-exponential decay, are plotted as a function of the total [d($T_4AT_5AT_4$)] in Figure 1B,C. The value of $k_{obs,1}$, increases linearly with increasing DNA concentration consistent with eq 4. The slope of the line in Figure 1B yields an estimate of the apparent bimolecular rate constant, k_1(app) = $(2.3 \pm 0.2) \times 10^7$ M^{-1} s^{-1}. Figure 1C shows that $k_{obs,2}$ increases hyperbolically with [d($T_4AT_5AT_4$)], consistent with eq 5 and Scheme 2. Based on eq 5, the plateau value of $k_{obs,2} = 8.5 \pm 1.0$ s^{-1} obtained at high [d($T_4AT_5AT_4$)] equals ($k_2 + k_{-2}$), the sum of the rate constants for the isomerization step in Scheme 2.

Kinetics of Rep Monomer Binding to Excess d(T_5(2-AP)-T_4(2-AP)T_5), Monitored by Enhancement of the DNA Fluorescence. We have also examined Rep monomer binding to ss DNA by monitoring a fluorescent probe on the DNA. These experiments were performed with the ss oligodeoxynucleotide, d(T_5(2-AP)T_4(2-AP)T_5), containing 2-aminopurine (2-AP), a fluorescent analogue of adenosine with the amino group at the 2-position rather than at the 6-position (Ward et al., 1969). This analogue is an excellent fluorescence probe to monitor DNA binding since it introduces only a nominal perturbation to the ss DNA. Furthermore, binding of Rep to d(T_5(2-AP)T_4(2-AP)T_5) results in a ~2-fold enhancement of the 2-AP fluorescence. The fluorescence emission spectrum of 2-aminopurine is red-shifted with respect to tryptophan with $\lambda_{ex,max}$ = 310 nm and $\lambda_{em,max}$ = 360 nm (Ward et al., 1969; Guest et al., 1991; Nordlund et al., 1993).

We performed a series of stopped-flow experiments mixing Rep (100 nM monomer) with d(T_5(2-AP)T_4(2-AP)T_5) (100 nM to 1 μM) (conditions that minimize Rep dimerization) while monitoring the enhancement of 2-AP fluorescence. Figure 2A shows representative stopped-flow traces from experiments performed at 100, 200, and 700 nM d(T_5(2-AP)T_4(2-AP)T_5). Since the concentration of fluorescent DNA is varied in these experiments, the fluorescence signal was normalized to the maximum fluorescence change for each experiment for ease of comparison. Each time course is well-described by a single-exponential decay with no further fluorescence changes at longer times (see time course at 100 nM Rep in Figure 7B). Figure 2B shows that the observed rate constant, k_{obs}, obtained from single-exponential fits of the experiments performed in excess d(T_5(2-AP)T_4-(2-AP)T_5), increases linearly with total DNA concentration over the range from 0.2 to 1.0 μM DNA. The linear least-squares slope of this line yields an apparent bimolecular rate constant, k_1(app) = $(2.8 \pm 0.7) \times 10^7$ M^{-1} s^{-1} (see eq 5). The intercept of the line in Figure 2B, 0.9 ± 0.4 s^{-1}, provides an estimate of the macroscopic rate constant for dissociation of DNA from both PS and PS* and equals $k_{-1}k_{-2}/(k_2 + k_{-2} + k_{-1})$ for the mechanism in Scheme 2 (see eq 5). Figure 2C shows that the overall enhancement of the 2-AP fluorescence upon binding Rep is constant at 1.7 ± 0.1 over the entire range of d(T_5(2-AP)T_4(2-AP)T_5) concentrations examined. This demonstrates that Rep monomer is saturated with ss DNA even at the lowest DNA concentrations examined (200 nM).

On the basis of the mechanism in Scheme 2, a single-exponential time course is expected under conditions of excess DNA if the fluorescence intensity of 2-AP is identical in the two species, PS and PS*. Thus the isomerization step, PS → PS*, is spectroscopically silent as monitored by 2-AP fluorescence. Recall that PS and PS* have different Trp fluorescence intensities, and thus biphasic kinetics are observed when monitoring Trp fluorescence even in experiments performed with a large excess of DNA (see Figure 1).

Kinetics of DNA-Induced Rep Dimerization. We next examined the kinetics of Rep binding to d(T_5(2-AP)T_4(2-AP)T_5) under conditions of excess Rep protein where significant Rep dimerization occurs. Figure 3A shows two kinetic time courses obtained from successive stopped-flow experiments on the identical sample by mixing an excess of Rep protein (300 nM monomer) with d(T_5(2-AP)T_4(2-AP)-T_5) (100 nM) in buffer A at 4.0 °C. In one reaction, we monitored the enhancement of DNA (2-AP) fluorescence (using λ_{ex} = 310 nm), whereas in the second reaction we monitored the quenching of the tryptophan fluorescence of Rep (using λ_{ex} = 290 nm). The amplitudes have been normalized to the maximum observed fluorescence changes to facilitate comparison of the two time courses. Although multiphasic at this high Rep concentration (300 nM), the time courses observed are nearly identical even though they are monitoring different spectroscopic signals. The first 5 s of each time course (left half of Figure 3A) reflecting DNA binding to the Rep monomer is biphasic. However, this is followed by a much slower third phase occurring over ~50 s (right half of Figure 3A), which is not observed in the experiments performed at the lower Rep concentration (100 nM) in the presence of excess DNA (Figures 1 and 2 and data not shown). Our previous studies have shown that Rep protein remains monomeric in the absence of DNA, even at 300 nM Rep, but is induced to dimerize upon binding DNA (Chao & Lohman, 1991; Wong et al., 1992; Wong & Lohman, 1992). As shown below, the third phase of the reaction reflects the slower kinetics of Rep dimer formation that is induced by binding ss DNA (see Figure 3B). Interestingly, both the 2-AP fluorescence of d(T_5(2-AP)T_4-(2-AP)T_5) and the intrinsic tryptophan fluorescence of Rep are influenced directly by Rep dimerization (additional enhancement of the 2-AP fluorescence and additional quenching of the tryptophan fluorescence).

Although the two time courses in Figure 3A are nearly identical, closer inspection indicates that the observed rate constant of the first phase obtained by monitoring the 2-AP (DNA) fluorescence is twice as fast as obtained by monitoring the Rep Trp fluorescence (10.5 ± 0.2 s^{-1} vs 4.9 ± 0.7 s^{-1}). This suggests that the first phase observed by Trp fluorescence quenching monitors a step that is slightly slower than the first step reported by the 2-AP fluorescence. However, the observed rate constant for the third phase, $k_{obs,3}$, is the same, regardless of which fluorescence signal is monitored, with $k_{obs,3}$(2-AP) = 0.095 ± 0.001 and $k_{obs,3}$(Trp) = 0.101 ± 0.001. (The value of $k_{obs,3}$(Trp) = 0.101 ± 0.001 was obtained after accounting for a slow steady state photobleaching of the tryptophan fluorescence.)

To estimate the rate constant for Rep dimerization, we examined the dependence of $k_{obs,3}$ on Rep concentration using 25 nM d(T_5(2-AP)T_4(2-AP)T_5) and excess Rep protein while monitoring the enhancement of 2-AP fluorescence. As shown in Figure 3B, $k_{obs,3}$ increases linearly with increasing

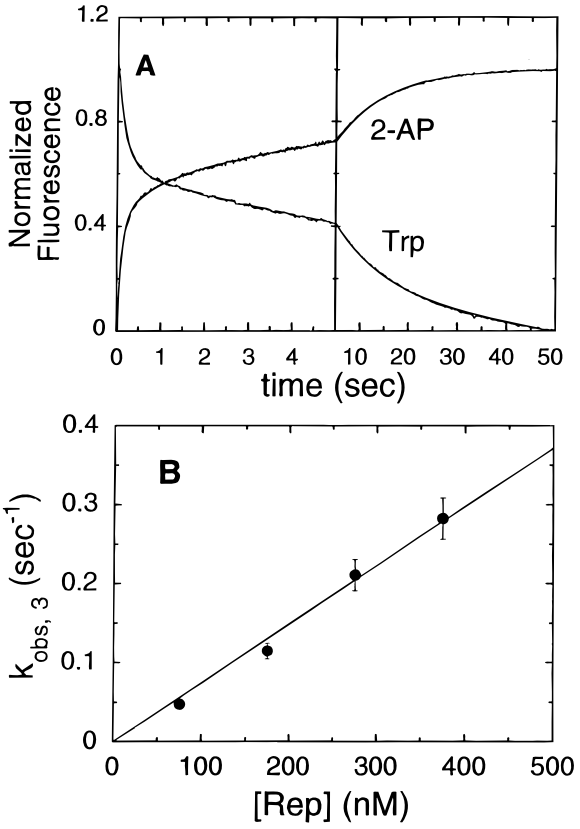

FIGURE 3: Kinetics of d(T_5(2-AP)T_4(2-AP)T_5) binding to an excess of Rep monomer displays multiphasic kinetics with the slowest phase reflecting Rep dimerization. A. Two stopped-flow kinetic time courses are shown for successive experiments performed on identical samples by mixing 300 nM Rep monomer with 100 nM d(T_5(2-AP)T_4(2-AP)T_5). One time course (Trp) monitors the quenching of the intrinsic Rep tryptophan fluorescence (λ_{ex} = 290 nm, λ_{em} > 320 nm), whereas the other time course (2-AP) monitors the enhancement of the 2-aminopurine fluorescence of the DNA (λ_{ex} = 315 nm, λ_{em} >350 nm). The time courses are displayed on a split time base to illustrate their multiphasic character and to more easily compare the time courses obtained by monitoring the different fluorophores. The biphasic kinetics within the first 5 s reflects the two-step binding of Rep monomer to the ss DNA shown in Scheme 2. The slow third phase reflects Rep dimerization (PS* + P → P_2S) shown in Scheme 3. Overlaid on the data is the fit to the sum of three exponentials. The observed rate constants from the nonlinear least-squares fits to the data are as follows: $k_{obs,1}$ = 10.5 ± 0.2 s^{-1}, $k_{obs,2}$ = 1.30 ± 0.05 s^{-1}, $k_{obs,3}$ = 0.095 ± 0.001 s^{-1}, for the 2-AP fluorescence and $k_{obs,1}$ = 4.93 ± 0.07 s^{-1}, $k_{obs,2}$ = 0.4 ± 0.2 s^{-1}, $k_{obs,3}$ = 0.100 ± 0.001 s^{-1}. The simulation of the time course of the Trp fluorescence change required an additional linear term (−0.002 V/s) to account for the slow photobleaching of the tryptophan fluorescence. B. Dependence on total Rep monomer concentration of the observed rate constant for the third slow phase, $k_{obs,3}$, monitored by the enhancement of the DNA (2-AP) fluorescence upon mixing 25 nM d(T_5(2-AP)T_4(2-AP)T_5) with the indicated concentration of excess Rep protein. The linear least-squares fits to the data, constrained to pass through the origin, has a slope of (7.4 ± 0.4) × 10^5 M^{-1} s^{-1}.

[Rep] in the range from 75 to 375 nM Rep. The slope of the linear least-squares line yields an apparent bimolecular rate constant for Rep dimerization of (7.4 ± 0.4) × 10^5 M^{-1} s^{-1} and an intercept that is indistinguishable from zero. The value of $k_{obs,3}$ in Figure 3B is proportional to [Rep] rather than to [Rep]^2 because Rep dimerization occurs only after DNA binding (Chao & Lohman, 1991; Wong et al., 1992; Wong & Lohman, 1992), and thus formation of the half-ligated Rep dimer, P_2S, is being monitored under conditions of excess Rep protein. The P_2S dimer is also favored at equilibrium under these conditions because of the negative

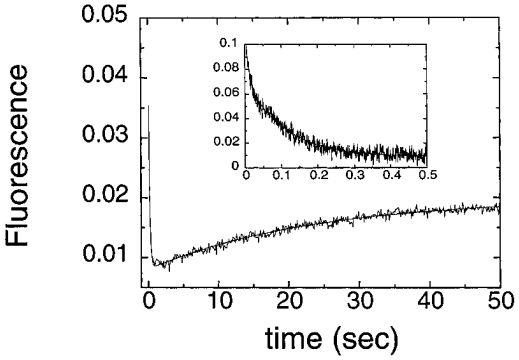

FIGURE 4: Kinetic evidence for negative cooperativity for ss DNA binding to the Rep dimer. A stopped-flow kinetic time course obtained by monitoring the quenching of Rep tryptophan fluorescence upon mixing Rep (300 nM monomer) with an excess of dT-$(pT)_{15}$ (5.0 μM). Under these conditions (buffer A, 4 °C) all of the Rep monomer is initially saturated with DNA within the first 500 ms (inset), which shows the Trp quenching reflecting Rep monomer binding and subsequent isomerization. (The solid curve is the best fit of this time course to a sum of two exponentials with $k_{obs,1}$=130 $\pm$ 10 s^{-1} and $k_{obs,2}$ = 9.5 $\pm$ 0.2 s^{-1}). After the initial saturation of the Rep monomer with $dT(pT)_{15}$, a slow net loss of bound dT-$(pT)_{15}$ occurs reflecting Rep dimerization (due to the negative cooperativity for DNA binding). The slow recovery of tryptophan fluorescence intensity occurring over the next 50 s occurs with observed rate constant, $k_{obs,3}$ = 0.054 $\pm$ 0.001 s^{-1}.

Scheme 3

$$2P + S \underset{k_{-1}}{\overset{k_1}{\rightleftharpoons}} PS + P \underset{k_{-2}}{\overset{k_2}{\rightleftharpoons}} PS^* + P \underset{k_{-3}}{\overset{k_3}{\rightleftharpoons}} P_2S$$

cooperativity for ss DNA binding to the Rep dimer (Wong et al., 1992; Wong & Lohman, 1992). Incorporation of Rep dimerization into Scheme 2 yields Scheme 3 which assumes that only the PS* species can dimerize with P to form P_2S (see Discussion).

Kinetics of Rep Dimerization in Excess DNA Demonstrates Negative Cooperativity for ss DNA Binding to the Rep Dimer. Under the conditions of our experiments (buffer A, 4.0 °C), there is an extreme negative cooperativity associated with ss DNA binding to the Rep dimer (Wong & Lohman, 1992). As a result, the half-ligated P_2S dimer is more stable than the P_2S_2 dimer at equilibrium. On the basis of these considerations, we designed a kinetic experiment to test directly for this negative cooperativity. We performed a stopped-flow experiment in which a high Rep monomer concentration (300 nM) was mixed with a large excess of $dT(pT)_{15}$ (5.0 μM), and the change in Rep tryptophan fluorescence was monitored. At these concentrations, the Rep monomer will become transiently saturated with dT-$(pT)_{15}$ to form a mixture of (PS + PS*), which should be followed by a net dissociation of $dT(pT)_{15}$ due to the slow redistribution to form P_2S at equilibrium. The time course of this experiment is shown in Figure 4. The inset to Figure 4 shows a rapid biphasic quenching of Trp fluorescence within the first 500 ms, which reflects Rep monomer−dT-$(pT)_{15}$ binding and isomerization. This is followed by a slow enhancement of Trp fluorescence, occurring over the next 50 s, reflecting net dissociation of $dT(pT)_{15}$. This slow phase occurs over the same time domain as is expected for Rep dimerization under conditions of excess Rep monomer. This directly demonstrates the extreme negative cooperativity for ss DNA binding to the Rep dimer. At this point, we cannot determine whether the pathway for this process goes through a P_2S_2 intermediate or whether it involves transient dissociation of DNA to form P, followed by the reaction P + PS → P_2S, although on the basis of the slow rate of dimerization to form P_2S_2 (I. Wong and T. M. Lohman, submitted), the latter pathway is more likely.

Use of Fluorescein-Labeled $dT(pT)_{15}$ to Monitor DNA Binding in Excess Rep. As an additional probe of Rep−DNA binding and dimerization we examined Rep binding to $dT(pT)_{15}$ that is modified with fluorescein at the 3′-end (3′-F-$dT(pT)_{15}$) as described previously (Bjornson et al., 1994). Fluorescein has its fluorescence excitation maximum at 497 nm and its emission maximum at 524 nm (Bjornson et al., 1994) and, when attached to $dT(pT)_{15}$, undergoes changes in its fluorescence intensity upon binding Rep. One advantage of fluorescein-labeled DNA over the DNA containing 2-AP is the much higher quantum yield of fluorescein that allows reactions to be monitored at DNA concentrations as low as 1 nM (Bjornson et al., 1994).

Figure 5 shows representative stopped-flow time courses monitoring the complex changes in fluorescein fluorescence upon mixing 300 nM Rep monomer with 5 nM 3′-F-dT-$(pT)_{15}$ (buffer A, 4.0 °C). As shown in Figure 5A, a rapid quenching of fluorescein fluorescence (~23%) occurs within the first 100 ms, which is followed by an enhancement of fluorescein fluorescence of approximately equal amplitude. These transients are followed by a third slow phase, corresponding to a quenching of fluorescein fluorescence, occurring over the next 50 s as shown in Figure 5B. The entire time course for 3′-F-$dT(pT)_{15}$ binding to Rep is well described by a sum of three exponential terms with an overall fluorescein fluorescence quenching of only ~4%. However, each successive phase is accompanied by changes in fluorescence intensity of opposite sign with time constants that are well-separated in time, thus all three phases are easily resolved.

The dependencies on [Rep] of the observed rate constants for each phase are shown in Figure 5 (panels C−E) and are consistent with the mechanism in Scheme 3. The rate constant for the first phase, $k_{obs,1}$, increases linearly with total Rep concentration, consistent with this phase reflecting the Rep−DNA binding. The linear least squares slope of the line in Figure 5C yields an apparent bimolecular rate constant of k_1(app) = (6.0 $\pm$ 0.7) × 10^7 M^{-1} s^{-1}. The intercept of the line in Figure 5C is 5 $\pm$ 1 s^{-1}, which equals (k_{-1} + k_2 + k_{-2}) according to eq 4. The dependence of $k_{obs,2}$ on [Rep] (Figure 5D) is hyperbolic with a plateau value of 3.8 $\pm$ 0.6 s^{-1}, corresponding to the sum of the rate constants (k_2 + k_{-2}) in Scheme 3. Therefore, the difference between the intercept of $k_{obs,1}$ and the plateau value of $k_{obs,2}$ provides an estimate of k_{-1} = 1.2 $\pm$ 1 s^{-1}. The rate constant for the third phase, $k_{obs,3}$, increases approximately linearly with [Rep] yielding an apparent bimolecular rate constant for Rep dimerization, k_3 = (3.3 $\pm$ 0.2) × 10^5 M^{-1} s^{-1}. Thus, the three phases appear to reflect DNA binding to the Rep monomer, isomerization to form PS*, and dimerization of PS* with excess P to form P_2S, respectively. The results from all three fluorescence probes, fluorescein, Trp, and 2-AP, are complementary and support Scheme 3 as the minimal mechanism for Rep-ss DNA binding and subsequent dimerization.

Kinetics of ss DNA Dissociation from Rep Dimers. To probe the mechanism of ss DNA dissociation from the singly ligated Rep dimer (a P_2S complex), we examined the kinetics of dissociation of a fluorescently labeled ss oligodeoxy-

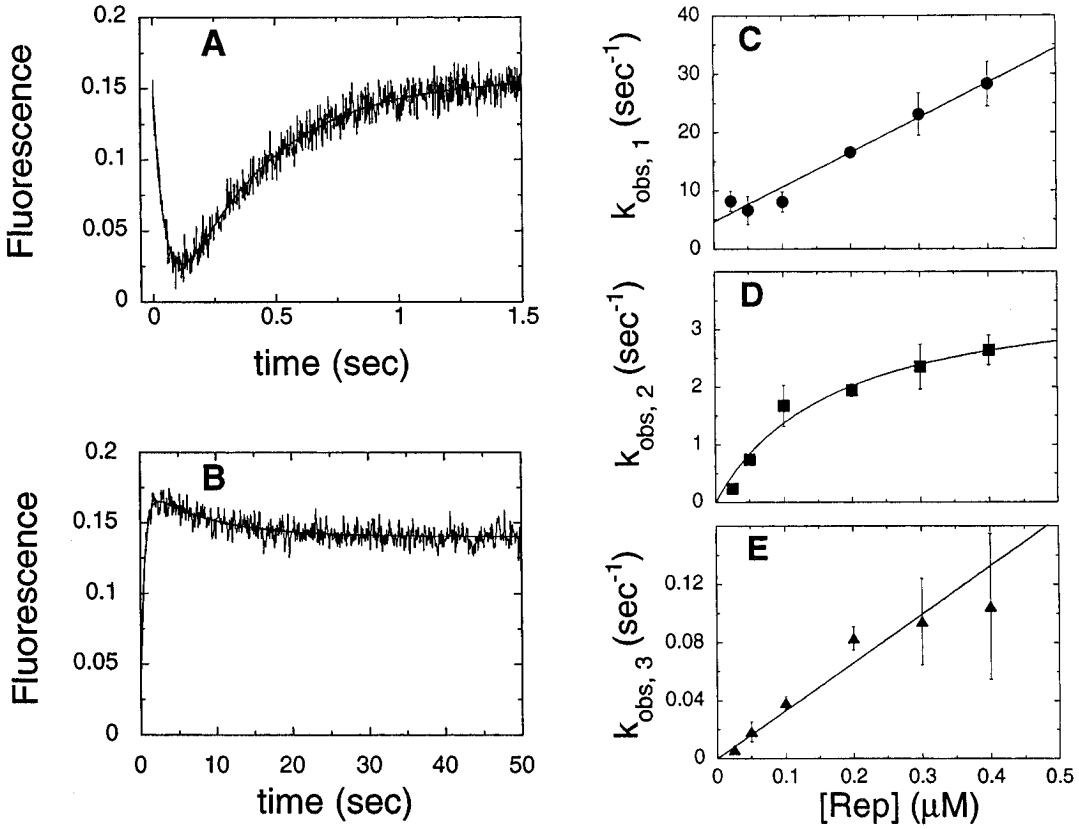

FIGURE 5: Three distinct kinetic phases are observed for fluorescein-labeled ss DNA (3′-F-dT(pT)$_{15}$) binding to excess Rep monomer. A. The first 1.5 s of the time course of fluorescein fluorescence (λ_{ex} = 492 nm, λ_{em} > 520 nm) upon mixing 5 nM 3′-F-dT(pT)$_{15}$ with 300 nM Rep monomer can be described by a sum of two exponentials, with the first phase ($k_{obs,1}$) occurring with a fluorescence quenching and the second phase ($k_{obs,2}$) a fluorescence enhancement. The values of $k_{obs,1}$ and $k_{obs,2}$ are plotted as a function of total Rep monomer concentration in panels C and D. B. The time course of the same reaction in panel A is shown over 50 s. The trace has been fit independently to a sum of two exponentials where only the third, slow phase ($k_{obs,3}$) is well defined. The Rep concentration dependence of $k_{obs,3}$ is plotted in panel E. C. The observed rate constant, $k_{obs,1}$ (●), describing the initial fluorescein fluorescence quenching is plotted as a function of total Rep monomer concentration. The linear least-squares line describing the data has a slope of (6.0 ± 0.7) × 10^7 M^{-1} s^{-1} and an intercept of 5 ± 1 s^{-1}. D. The observed rate constant, $k_{obs,2}$ (■), describing the second phase, corresponding to a relative fluorescein fluorescence enhancement, is plotted as a function of total Rep monomer concentration. The data have been fitted to a square hyperbola with a zero intercept, apparent K_d of 0.17 ± 0.05 μM, and a plateau value of 3.8 ± 0.6 s^{-1}. E. The observed rate constant, $k_{obs,3}$ (▲), describing the third phase, corresponding to a relative fluorescein fluorescence quenching, is plotted as a function of total Rep monomer concentration. The data have been fitted to a straight line with a zero intercept and a slope of (3.3 ± 0.2) × 10^5 M^{-1} s^{-1}, using weighted least squares.

nucleotide (S) bound to the Rep dimer upon addition of an excess of a nonfluorescent ss DNA competitor (C). The singly ligated Rep dimer, P_2S, was formed by preincubating 100 nM d(T_5(2-AP)T_4(2-AP)T_5) with 300 nM Rep (final concentrations) in buffer A at 4.0 °C. This P_2S complex was then mixed with an excess of d($T_5AT_4AT_5$) in the stopped-flow, and the net dissociation of (d(T_5(2-AP)T_4(2-AP)T_5)) was monitored by the resulting decrease in 2-AP fluorescence. Figure 6A shows a series of time courses obtained upon mixing P_2S with different competitor DNA concentrations ranging from 1 to 50 μM d($T_5AT_4AT_5$). Each dissociation time course is very slow and well described by a single-exponential decay (the single-exponential fits are overlaid on the data). With the exception of the lowest concentration of competitor DNA (1.0 μM) (Figure 6A and data not shown), the amplitudes of the single-exponential time courses are all constant, demonstrating that the competitor DNA completely displaces the prebound d(T_5(2-AP)T_4-(2-AP)T_5) at equilibrium. However, Figure 6B shows that the observed rate constant, $k_{obs,diss}$, for net dissociation of S, increases hyperbolically with increasing competitor DNA concentration from a value of 0.0035 ± 0.0002 s^{-1} at 1.0 μM d($T_5AT_4AT_5$) to a value of 0.0059 ± 0.0002 s^{-1} at 50 μM d($T_5AT_4AT_5$). This dependence of $k_{obs,diss}$ on competitor [DNA] demonstrates that the competitor DNA (C) binds to the P_2S complex to transiently form a doubly ligated P_2SC intermediate. However, the rate of C binding to the free subunit of the P_2S dimer is slow; in fact, the net rate of dissociation of S from P_2S is partially limited by the binding of competitor DNA.

The hyperbolic dependence of $k_{obs,diss}$ on competitor [DNA] can be explained by the mechanism in Scheme 4. The observed rate constant for DNA dissociation from P_2S in the absence of competitor DNA is 0.0032 ± 0.0001 s^{-1} as determined from the intercept of the plot in Figure 6B. As discussed below, the preferred pathway for this process (vertical pathway in Scheme 4) is by dissociation of the P_2S dimer to form P + PS*, which is rate limiting, followed by more rapid dissociation of S from PS*. The rate-limiting step for this process is k_{-3} (see Scheme 4), and thus k_{-3} = 0.0032 ± 0.0001 s^{-1}. However, in the presence of a large excess of competitor DNA (C), net dissociation of S occurs by the horizontal pathway in Scheme 4 through transient formation of the doubly ligated Rep dimer, P_2SC.

In the presence of competitor DNA, dissociation of S from the Rep dimer is a two-step reaction, with binding of competitor DNA preceding DNA dissociation. The observed rate constant for dissociation of S from P_2SC, $k_{obs,diss}$, is given by the plateau value at high competitor [DNA] (see Figure 6). However, as shown in Scheme 4, there are two possible

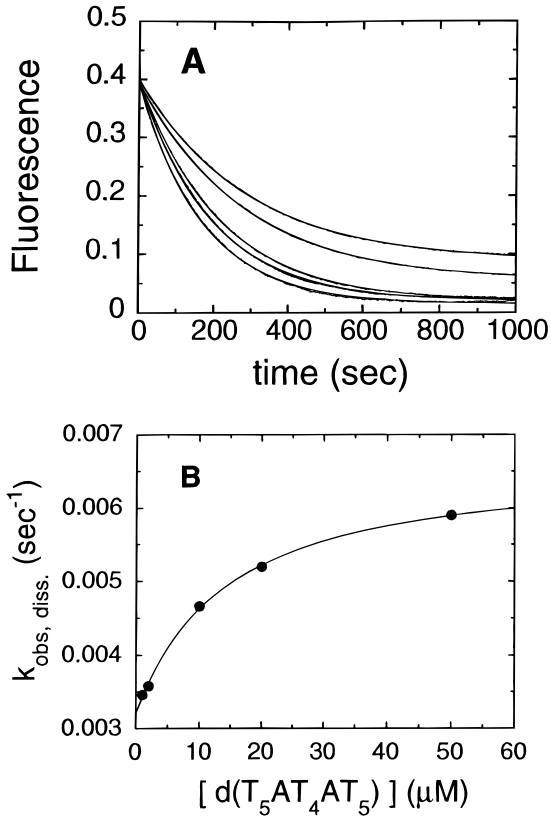

FIGURE 6: Observed rate constant for ss oligodeoxynucleotide dissociation from the singly ligated Rep dimer, P_2S, increases with concentration of competitor DNA. A. The singly ligated Rep dimer, P_2S, was formed by preincubating 100 nM d(T_5(2-AP)T_4(2-AP)-T_5) with 300 nM Rep (final concentrations) in buffer A (4.0 °C). This was then mixed in a stopped-flow experiment with a large excess of the nonfluorescent oligodeoxynucleotide d($T_5AT_4AT_5$), and the loss of fluorescence associated with the net dissociation of d(T_5(2-AP)T_4(2-AP)T_5) was monitored. Time courses from five experiments performed at different competitor [DNA] are shown. Each time course was fit to a single-exponential decay, with observed rate constant, $k_{obs,diss}$, and the simulated time course is overlaid on each set of data. B. The observed dissociation rate constant, $k_{obs,diss}$, is plotted as a function of the total competitor DNA concentration. The data are well described by a square hyperbola with an intercept of 0.0032 ± 0.0005 s^{-1}, an apparent K_d of 14 ± 2 μM, and a final plateau value of 0.0067 ± 0.0005 s^{-1}.

Scheme 4

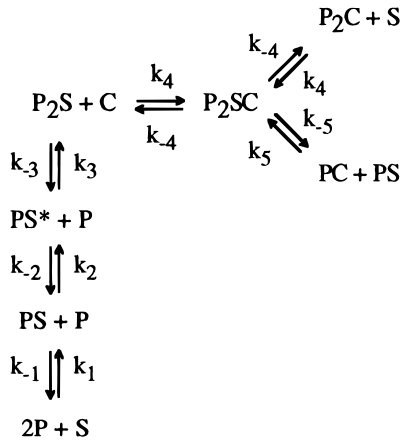

pathways for dissociation of S from P_2SC: direct dissociation to form P_2C + S (with rate constant k_{-4}) or dissociation of the P_2SC dimer to form PS* + PC* (with rate constant k_{-5}), followed by rapid dissociation of S from PS*. Therefore, the observed rate constant for net dissociation of S from P_2-SC, $k_{obs,diss}$ = 0.0067 ± 0.0002 s^{-1} = k_{-4} + k_{-5}. Although the data in Figure 6 do not allow us to determine the relative contributions of these two pathways, experiments with a cross-linked Rep monomer−d($T(pT)_{15}$ complex have determined a value of k_{-5} = 0.0069 ± 0.0001 s^{-1} for P_2S_2 dissociation under these same solution conditions (I. Wong and T. M. Lohman, submitted). This indicates that the dominant pathway for dissociation of S from P_2SC under these solution conditions is pathway 5, with k_{-5} = 0.0067 ± 0.0002 s^{-1}.

Analysis of the hyperbolic dependence of $k_{obs,diss}$ on competitor [DNA] in Figure 6B, yields a lower limit of k_4 ≥ 250 M^{-1} s^{-1} for the apparent bimolecular rate constant for C binding to P_2S (see Scheme 4). This apparent bimolecular rate constant is lower by a factor of ~10^6 than the value expected for a diffusion-controlled reaction. It is also lower by nearly a factor of ~10^5 than the apparent bimolecular rate constant, k_1(app) = 3 × 10^7 M^{-1} s^{-1}, that we have measured for the same ss DNA binding to the Rep monomer (P). Therefore this value of k_4 ≥ 250 M^{-1} s^{-1} does not reflect the actual rate constant for the bimolecular binding reaction. The fit of the data in Figure 6B to a hyperbola also provides a lower limit estimate of K_4 = 0.07 μM^{-1} for the equilibrium constant for binding of C to the unfilled DNA binding site of P_2S (see Scheme 4).

Determination of the Elementary Rate Constants by Global Analysis of d(T_5(2-AP)T_4(2-AP)T_5) Binding to Rep. The experiments described above were performed under conditions that were close to pseudo first order in either Rep or DNA in order to simplify the analysis and provided estimates of most of the rate constants in Scheme 3 (except for k_{-1} and k_{-2}). However, some of these estimates required the use of different oligodeoxynucleotides while monitoring different fluorescent probes (tryptophan, 2-aminopurine, or fluorescein). Since the values of some of these rate constants are likely to be sensitive to the particular DNA used, we wished to determine values for the complete set of rate constants, including k_{-1} and k_{-2}, for the mechanism given in Scheme 3 using a single oligodeoxynucleotide. This requires a set of kinetic experiments performed over a range of Rep and DNA concentrations including some at comparable concentrations in order to obtain sufficient information on all the species in Scheme 3 and the rate constants governing their formation and decay. Since such a set of experiments cannot be analyzed analytically, the entire set of kinetic time courses was analyzed simultaneously (globally) by nonlinear regression using the program FITSIM (Zimmerle & Frieden, 1989) to obtain a consistent set of rate constants and their error estimates. A further advantage of such global analysis is that the amplitudes of the fluorescence changes are also included in the analysis, providing additional constraints on the determination of the kinetic rate constants.

A series of 10 stopped-flow experiments was performed at a constant concentration (100 nM) of the fluorescent DNA, d(T_5(2-AP)T_4(2-AP)T_5), and six Rep monomer concentrations varying from 25 to 400 nM, and the increase in 2-AP fluorescence was monitored. A wavelength of 315 nm was used to excite the 2-AP fluorescence, in order to minimize excitation of tryptophan, and fluorescence intensity was monitored using a 350 nm cut-on filter. To verify that only changes in 2-AP fluorescence intensity were being monitored, a control experiment was performed (λ_{ex} = 315 nm)

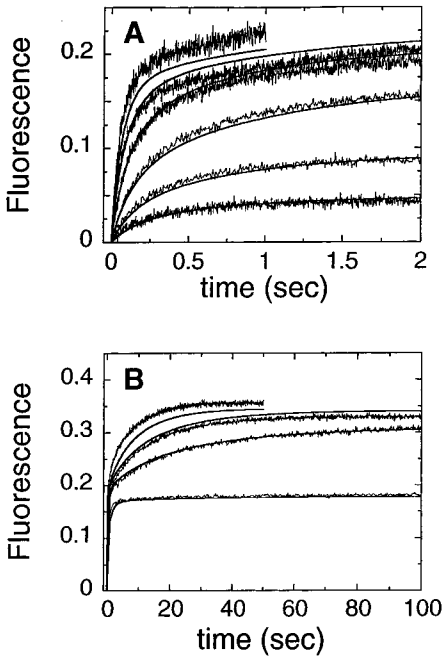

FIGURE 7: Simultaneous (global) analysis of kinetic time courses for d(T_5(2-AP)T_4(2-AP)T_5) binding to Rep monomer. The stopped-flow kinetic traces shown in panels A and B were performed with 100 nM d(T_5(2-AP)T_4(2-AP)T_5) and Rep monomer at six Rep concentrations (25−400 nM monomer) while monitoring the enhancement of the 2-aminopurine (2-AP) fluorescence of the DNA (λ_{ex} = 315 nm, λ_{em} > 350 nm). These data were simultaneously (globally) analyzed using the numerical analysis program FITSIM (Zimmerle & Frieden, 1989) to obtain the rate constants (and their associated uncertainties) for the mechanism given in Scheme 3 (see Table 1). This analysis was performed by constraining the relative enhancement of 2-AP fluorescence to the following values: 1.8 for (PS and PS*), and 2.4 for P_2S. The solid lines overlaying the data are the kinetic time courses simulated using the numerical kinetic simulation program KINSIM (Barshop et al., 1983), the kinetic mechanism in Scheme 3, the relative 2-AP fluorescence enhancements, and the rate constants in Table 1. A. Six stopped-flow kinetics traces showing the initial fast phases (first 2 s), reflecting primarily Rep monomer−DNA binding and isomerization, for experiments performed at a constant concentration of 100 nM dT_5(2-AP)T_4(2-AP)T_5. The concentrations of total Rep monomer are: 25 nM (lowest amplitude trace), 50, 100, 200, 300, and 400 nM (highest amplitude trace). B. Four stopped-flow kinetics traces showing the slower phases, reflecting Rep protein dimerization. The experiments were performed at a constant concentration of 100 nM dT_5(2-AP)T_4(2-AP)T_5. The concentrations of total Rep monomer are as follows: 100 nM (bottom trace), 200, 300, and 400 nM (top trace). For experiments performed at [Rep] ≤ 100 nM (conditions of excess DNA), no additional changes in 2-AP fluorescence are observed after the initial fluorescence signal changes shown in panel A (data not shown).

by mixing 100 nM nonfluorescent DNA d($T_5AT_4AT_5$) with 400 nM Rep monomer. In this control, no fluorescence signal changes were observed indicating that there was no contribution to the observed signal due to changes in tryptophan fluorescence.

Global analysis of the ten stopped-flow kinetic time courses shown in Figure 7 was performed using FITSIM (Zimmerle & Frieden, 1989) by floating the six rate constants in Scheme 3, while constraining the relative enhancement of d(T_5(2-AP)T_4(2-AP)T_5) fluorescence for the various Rep−DNA species to the values that were determined independently and given in Table 1. The relative enhancement of d(T_5(2-AP)T_4(2-AP)T_5) fluorescence upon formation PS is 1.7 ± 0.1 as determined from Figure 2C, and there is no additional fluorescence change upon isomerization to form PS*. The 2-AP fluorescence enhancement upon formation of the P_2S dimer, relative to free DNA, was determined to be 2.4 ± 0.1, on the basis of independent equilibrium fluorescence titrations (see Figure 8A). The rate constants and their error estimates determined from the global analysis are given in Table 1. These estimates agree very well with those determined from the experiments performed under pseudo-first-order conditions. The solid curves overlaying the data in Figure 7 are the time courses simulated for Scheme 3 using the program KINSIM (Barshop et al., 1983) and the rate constants and fluorescence enhancement factors given in Table 1. Each individual kinetic trace is well described by the simulated timecourses. Only slight deviations are observed for the experiments performed at the two highest Rep concentrations (300 and 400 nM Rep). This is due to the fact that a constant output factor, which relates the concentration of each species (S, PS, PS*, and P_2S) to its fluorescence intensity, was used to simulate each kinetic time course in the global analysis. However, this deviation is eliminated by only a 4% change in the value of the output factor, which is well within our error limits. The excellent agreement between these simulations and the actual time courses provides further support for Scheme 3.

Equilibrium Titrations of d(T_5(2-AP)T_4(2-AP)T_5) with Rep Monitoring 2-AP Fluorescence. Equilibrium binding of Rep to d(T_5(2-AP)T_4(2-AP)T_5) was examined by titrating d(T_5(2-AP)T_4(2-AP)T_5) with Rep (buffer A at 4.0 °C) and monitoring complex formation by the enhancement of 2-AP fluorescence. The 2-AP fluorescence was excited at 310 nm (filled symbols) or 315 nm (open circles) and the fluorescence emission intensity was monitored using the same cut-on filter (>350 nm) used in the stopped-flow experiments. The overall enhancement of 2-AP fluorescence relative to free oligodeoxynucleotide is 2.4 ± 0.1 for excitation at 315 nm and 3.0 ± 0.1 for excitation at 310 nm. The results of three such titrations performed at 100, 200, and 400 nM d(T_5(2-AP)T_4(2-AP)T_5) are shown in Figure 8. The solid lines in Figure 8 are simulations of the fluorescence titrations based on Scheme 5, the equilibrium constants, K_1, K_2, and K_3, reported in Table 1, and K_4 = 0.07 μM^{-1}.[1] These equilibrium constants provide a good description of the equilibrium titrations at all three DNA concentrations including the d(T_5(2-AP)T_4(2-AP)T_5) concentration (100 nM) used in the stopped-flow experiments shown in Figure 7. Figure 8B shows the population distribution of Rep species at 100 nM d(T_5(2-AP)T_4(2-AP)T_5) as a function of the total Rep monomer concentration which is predicted from these equilibrium constants. The fraction of the monomer species, PS, is small due to the thermodynamically favorable isomerization to form PS*. Under these titration conditions (low [DNA] and high [Rep]) the dominant Rep−DNA species at saturating Rep concentrations is the singly ligated Rep dimer P_2S; the doubly ligated Rep dimer species P_2S_2 is not detectably populated.

Dependence of the Steady State ATPase Activity on Rep Concentration is Consistent with the Rate Constants Determined by Stopped-Flow Experiments. The equilibrium constants obtained from the global kinetic analysis (Table 1) accurately predict the equilibrium fluorescence titrations in Figure 8A; however, the overall equilibrium constant for Rep monomer binding to d(T_5(2-AP)T_4(2-AP)T_5) [$K_1(1 + K_2)$ = 320 ± 170 μM^{-1}] is significantly larger than the equivalent equilibrium constant (K_{1S} = 2 ± 0.3 μM^{-1}) (see Scheme 1) determined previously using nitrocellulose filter binding under identical solution conditions (Wong & Lo-

Table 1: Rate and Equilibrium Constants Determined from a Global Analysis of Rep−d(T_5(2-AP)T_4(2-AP)T_5) Binding Kinetics According to Scheme 3 (Buffer A at 4 °C)[a]

step	$P + S \rightleftarrows PS$	$PS \rightleftarrows PS^*$	$PS^* + P \rightleftarrows P_2S$
$k_{forward}$	k_1(app) = (3.3 ± 0.5) × 10^7 M^{-1} s^{-1}	$k_2 = 2.7 \pm 0.9$ s^{-1}	$k_3 = (4.5 \pm 0.3) \times 10^5$ M^{-1} s^{-1}
$k_{reverse}$	$k_{-1} = 1.4 \pm 0.4$ s^{-1}	$k_{-2} = 0.21 \pm 0.06$ s^{-1}	$k_{-3} = 0.0027 \pm 0.0008$ s^{-1}
K_{eq}	$K_1 = 23 \pm 7$ μM^{-1}	$K_2 = 13 \pm 6$	$K_3 = 170 \pm 50$ μM^{-1}
relative enhancement of 2-AP fluorescence[b]	1.7 ± 0.1	1.7 ± 0.1	2.4 ± 0.1

[a] Global analysis using FITSIM [Zimmerle & Frieden (1989)] was performed on the 10 sets of stopped-flow kinetic experiments shown in Figure 7 performed at 100 nM d(T_5(2-AP)T_4(2-AP)T_5) and total Rep monomer concentrations from 25 to 400 nM. [b] The enhancement of 2-AP fluorescence is relative to free d(T_5(2-AP)T_4(2-AP)T_5) and was determined independently (see Figures 2C and 8A).

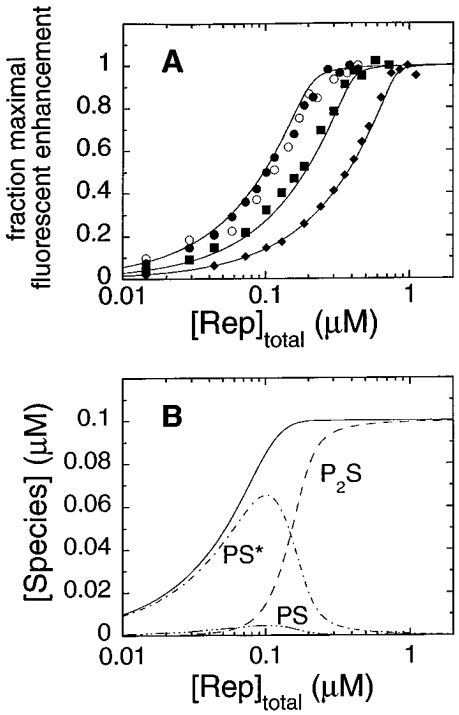

FIGURE 8: Equilibrium titrations of d(T_5(2-AP)T_4(2-AP)T_5) with Rep protein, monitoring the enhancement of 2-aminopurine (2-AP) fluorescence. A. Titrations of d(T_5(2-AP)T_4(2-AP)T_5) with Rep protein, monitoring the 2-AP fluorescence of d(T_5(2-AP)T_4(2-AP)-T_5) (λ_{ex} = 310 nm except as indicated, λ_{em} > 350 nm), were performed at 100 nM (●) (○, λ_{ex} = 315 nm), 200 nM (■), and 400 nM (◆) DNA. For each titration, the observed fluorescence emission intensity of each titration was normalized to the maximum observed fluorescence enhancement at saturation (3.0 ± 0.1 for λ_{ex} = 310 nm and 2.4 ± 0.1 for λ_{ex} = 315 nm). The curves overlaying the data are simulations based on Scheme 3, the kinetic rate constants in Table 1, and the relative 2-AP fluorescence enhancements of the monomer Rep−DNA species, PS and PS* (1.8) and singly ligated Rep dimer, P_2S (2.4). B. The population distribution of DNA-ligated Rep species predicted from Scheme 3 and the equilibrium constant (K_1, K_2, and K_3) given in Table 1 for 100 nM d(T_5(2-AP)T_4(2-AP)T_5) as a function of total Rep monomer concentration. Note that the solid line representing total DNA bound is not identical to the normalized fluorescence trace in panel A at the same DNA concentration (100 nM) due to the additional fluorescence enhancement of the P_2S dimer relative to the ligated monomers PS and PS*.

hman, 1992). However, the equilibrium constant, L_{2S}, for Rep dimerization to form P_2S determined by filter binding (Wong & Lohman, 1992) is the same within error as that determined from this kinetics study (K_3 in Table 1). We have repeated the filter binding experiments using both dT-$(pT)_{15}$ and d(T_5(2-AP)T_4(2-AP)T_5), and the resulting binding isotherms agree with those determined previously using dT-$(pT)_{15}$ (Wong et al., 1992) (data not shown).

To address the quantitative differences between the equilibrium constants determined by filter binding and those given in Table 1 and to assess which set of equilibrium constants provide a better description of the population distribution of Rep−DNA species we examined the steady state ATPase activity of Rep (initial velocities) at a series of [Rep] at constant [$dT(pT)_{15}$]. Since the different Rep monomer species [P, (PS + PS*)] and Rep dimer species (P_2S, P_2S_2) have very different ATPase activities (Moore & Lohman, 1994a; Wong et al., 1993; K. J. M. Moore, unpublished), the observed ATPase activity can be a very sensitive probe of the population distribution of the different Rep species. We chose a range of [Rep] for which the two sets of equilibrium constants predict very different distributions of Rep monomers vs dimers and initial velocities of ATP hydrolysis (μM ATP hydrolyzed s^{-1}) were measured at constant [$dT(pT)_{15}$] (1.0 μM) for a series of Rep concentrations (buffer A at 4.0 °C and 1 mM [α-^{32}P]ATP). These initial velocities should be a function of only the equilibrium distributions of the Rep−DNA species before the addition of ATP. The results are plotted in Figure 9 and are compared with the ATPase activity predicted using eq 3 and the equilibrium population of Rep−DNA species calculated using the equilibrium constants (K_1, K_2, and K_3) in Table 1 (solid line) or the equilibrium constants determined from nitrocellulose filter binding (dashed line) (Wong & Lohman, 1992). These results indicate that the equilibrium constants determined from the stopped-flow kinetic studies (see Table 1) provide a better description of the equilibrium population of Rep−$dT(pT)_{15}$ species. In particular, the ATPase activity predicted from the equilibrium constants in Table 1 show the same nonlinear dependence on [Rep] as is observed experimentally. The steady state values of k_{cat} used to simulate the ATPase activities were determined independently for each of the Rep−DNA species ((PS + PS*), P_2S, P_2S_2) (see Materials and Methods).[1]

DISCUSSION

A molecular understanding of the mechanism by which the dimeric Rep helicase unwinds duplex DNA requires knowledge of the rate constants for each step of the mechanism and how each step is coupled to ATP binding and hydrolysis. It is therefore necessary to determine the kinetic mechanism of DNA binding (both ss and ds DNA to Rep monomer and both subunits) and DNA-induced Rep dimerization. This is important since Rep initiates unwinding *in vitro* at a 3′-ss DNA flanking the duplex (Amaratunga & Lohman, 1993), and switching of Rep subunits bound to ss vs ds DNA has been proposed to be involved in the active, rolling mechanism of Rep-catalyzed DNA unwinding (Wong & Lohman, 1992). Furthermore, Rep dimerization has been implicated as a rate-limiting step in the pre-steady state kinetics of Rep-catalyzed DNA unwinding (Bjornson et al., 1994). Therefore, we have performed transient stopped-flow

Scheme 5

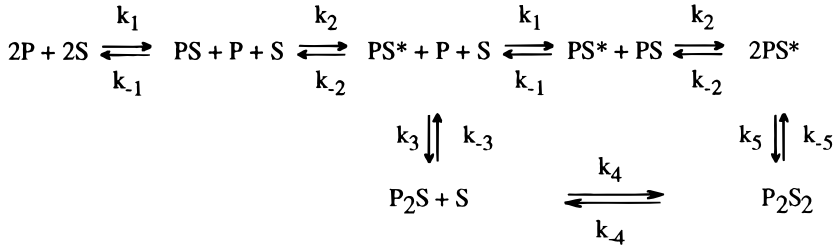

kinetic studies to determine a minimal mechanism and the rate constants for Rep monomer binding to ss oligodeoxynucleotides and subsequent Rep dimerization.

Minimal Kinetic Mechanism for ss DNA Binding to Rep Monomers and Subsequent Rep Dimerization. As in our previous equilibrium studies (Wong et al., 1992; Wong & Lohman, 1992), the kinetic studies described here were performed with ss oligodeoxynucleotides ($dN(pN)_{15}$) that are short enough so that each DNA can bind to only one Rep monomer or subunit of the dimer. Use of such oligodeoxynucleotides facilitates resolution of the kinetic rate constants for DNA binding from those of Rep dimerization. Based on these stopped-flow experiments, Scheme 3 is the minimal kinetic mechanism describing $dN(pN)_{15}$ binding to Rep monomer and subsequent dimerization to form the singly ligated Rep dimer, P_2S. In fact, Scheme 3 is consistent with the results of experiments performed with three different fluorescent probes: the intrinsic Rep tryptophan as well as DNA that either contained 2-aminopurine or that was 3′-end-labeled with fluorescein. Therefore, the steps outlined in Scheme 3 are independent of the particular fluorescent probe that was monitored and are not artifacts of these fluorescent probes. However, the quantitative estimates of some of the rate constants are dependent upon which probe is monitored. The results of our kinetic studies indicate that Rep monomer binds ss DNA via a two-step mechanism: a rapid bimolecular association step to form PS [$(3-6) \times 10^7$ $M^{-1}s^{-1}$], followed by an isomerization to form PS* ($3-8$ s^{-1}). At sufficiently high Rep concentrations, this is followed by a slower Rep dimerization step to form the P_2S complex [$(3-7) \times 10^5$ $M^{-1}s^{-1}$]. The half-ligated Rep dimer, P_2S, is favored under the conditions of our experiments due to the strong negative cooperativity that exists for DNA binding to the Rep dimer under these conditions (5 mM Mg^{2+}, pH 7.5, 4.0 °C) as observed previously in equilibrium binding studies (Wong et al., 1992; Wong & Lohman, 1992) and confirmed by our kinetic results (Figures 4 and 6).

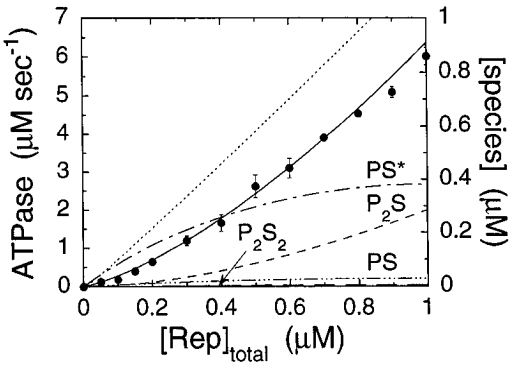

FIGURE 9: Steady state ATPase activity as a function of the total Rep monomer concentration at constant $[dT(pT)_{15}]$. ATPase activities, measured as initial velocities, were determined at 1.0 μM $dT(pT)_{15}$ and 1 mM [^{32}P]ATP at varying total Rep concentrations (right axis) in buffer A at 4.0 °C. The solid line is the predicted ATPase activity at each Rep concentration based on the equilibrium distribution of Rep−DNA species shown that are predicted from the equilibrium constants (K_1, K_2, and K_3) that were calculated from the kinetic rate constants for Scheme 3 given in Table 1 and the known values of k_{cat} for the individual Rep species (see Materials and Methods). The dashed line shows the initial ATPase velocities predicted using the distribution of Rep−DNA species using the equilibrium constants determined previously (Wong & Lohman, 1992) and the same values of k_{cat}.

The experiments reported here were performed at 4 °C (buffer A) for two reasons. The first was to enable quantitative comparisons with the Rep−DNA equilibrium binding constants and dimerization constants obtained previously (Wong et al., 1992; Wong & Lohman, 1992). These are also the same conditions that were used to examine the kinetic mechanism of nucleotide binding to and hydrolysis by the Rep monomer (Moore & Lohman, 1994a,b). The second reason was that this low temperature facilitates quantitative kinetic studies since it lowers the rate of Rep−ss DNA binding into a range that is more easily measured. However, preliminary stopped-flow studies performed at 25 °C indicate that the qualitative features of the mechanism in Scheme 3 [i.e., biphasic tryptophan quenching upon binding $dT(pT)_{15}$] also hold at the higher temperatures (15 and 25 °C) under which DNA unwinding has been examined (Amaratunga & Lohman, 1993; Bjornson et al., 1994).

The results reported here provide direct evidence for an isomerization step (PS → PS*) following the initial binding of ss DNA to the Rep monomer. Although this has not been observed previously, it is not unexpected in light of the fact that Rep dimerization is induced by DNA binding (Chao & Lohman, 1991; Wong et al., 1992; Wong & Lohman, 1992). Rep exists exclusively as a stable monomer in solution, even at concentrations up to its solubility limit; however, DNA binding induces Rep monomer to adopt a conformation that facilitates high-affinity dimerization (170 ± 50 μM^{-1}). This isomerization step probably reflects a major conformational change in the Rep monomer that is needed for Rep dimerization since we observe it in independent experiments monitoring fluorescence probes on the DNA (fluorescein) and the protein (tryptophan) as well as indirectly from global analysis of the 2-AP experiments. However, that PS* is required for Rep dimerization remains an assumption in the mechanism in Scheme 3. On the other hand, even if PS can also dimerize, inclusion of this pathway does not affect our analysis of the kinetics of Rep dimerization since isomerization is rapid on the time scale of dimerization and PS only represents ~7% of the total population of (PS + PS*). An adequate test of whether PS can also dimerize will require solution conditions under which PS is more highly populated (i.e., a lower value of K_2).

Initially it might seem surprising that the global analysis of the kinetics of Rep binding to $d(T_5(2\text{-AP})T_4(2\text{-AP})T_5)$ is sensitive to the isomerization step in Scheme 3 because the

Table 2: Rate Constants Determined According to Scheme 3 by Monitoring Different Fluorescent Probes (Buffer A, 4 °C)

fluorescent probe	tryptophan	fluorescein	2-AP[a]	
SS DNA	$dT_5AT_4AT_5$	3′-F-$dT(pT)_{15}$	$d(T_5(2\text{-AP})T_4(2\text{-AP})T_5)$[a]	$d(T_5(2\text{-AP})T_4(2\text{-AP})T_5)$[b]
k_1(app) (M^{-1} s^{-1})	$(2.3 \pm 0.2) \times 10^7$	$(6.0 \pm 0.7) \times 10^7$	$(2.8 \pm 0.7) \times 10^7$	$(3.3 \pm 0.5) \times 10^7$
k_{-1} (s^{-1})	ND[c]	1.2 ± 1	ND	1.4 ± 0.4
$k_2 + k_{-2}$ (s^{-1})	8.5 ± 1.0	3.8 ± 0.6	ND	2.9 ± 0.9
k_3 (M^{-1} s^{-1})	ND	$(3.3 \pm 0.2) \times 10^5$	$(7.4 \pm 0.4) \times 10^5$	$(4.5 \pm 0.3) \times 10^5$
k_{-3} (s^{-1})	ND	ND	0.0032 ± 0.0005[d]	0.0027 ± 0.0008

[a] Rate constants estimated from experiments performed under conditions of excess Rep or excess DNA. [b] Rate constants determined by global analysis of data in Figure 7A,B (see Table 1). [c] Not determined. [d] The intercept value in Figure 6B (see Results).

2-AP fluorescence intensities of PS and PS* are identical (see Figure 2A). However, global analysis of the binding data shown in Figure 7A is able to resolve the kinetic rate constants for this step (Table 1). This is due to the fact that isomerization leads to a significantly higher affinity of Rep monomer for ss DNA, resulting in a time-dependent enhancement of 2-AP fluorescence that is coupled to isomerization at low Rep concentrations. Attempts to fit the time courses in Figure 7 with a mechanism that does not include this isomerization step resulted in significantly poorer fits with systematic deviations at the shorter times that are sensitive to DNA binding (data not shown).

Comparison of Rate Constants Determined by Monitoring Different Fluorescence Probes. Although the kinetic mechanism in Scheme 3 is supported qualitatively by all of the stopped-flow experiments, there are quantitative differences in some of the rate constants, depending on the fluorescence probe used. The rate constants determined from experiments performed under pseudo-first-order conditions monitoring Rep Trp or DNA fluorescein fluorescence are listed in Table 2. One quantitative difference among these data is the estimate of k_1(app), the apparent bimolecular rate constant for Rep monomer binding to the ss oligodeoxynucleotide. The value of $k_1(\text{app}) = (3.3 \pm 0.5) \times 10^7$ M^{-1} s^{-1}, obtained from global fitting to Scheme 3 of the Rep−$d(T_5(2\text{-AP})T_4(2\text{-AP})T_5)$ data (see Table 1), agrees with the estimate of $(2.8 \pm 0.7) \times 10^7$ M^{-1} s^{-1} obtained from experiments with the same ss DNA but performed under pseudo-first-order conditions ([DNA] ≫ [Rep]). However, an estimate of $k_1(\text{app}) = (6.0 \pm 0.7) \times 10^7$ M^{-1} s^{-1} was obtained by monitoring the initial quenching of fluorescein (F) fluorescence upon binding 3′-F-$dT(pT)_{15}$ to Rep monomer under pseudo-first-order conditions of excess Rep (Figure 5). Furthermore, an estimate of $k_1(\text{app}) = (2.3 \pm 0.2) \times 10^7$ M^{-1} s^{-1} was obtained for $d(T_5AT_4AT_5)$ binding to Rep monomer by monitoring Rep tryptophan fluorescence quenching under pseudo-first-order conditions of excess DNA (Figures 1A, 3A, and 4).

The estimate of $k_1(\text{app}) = (6.0 \pm 0.7) \times 10^7$ M^{-1} s^{-1} obtained from monitoring fluorescein (F) fluorescence quenching upon binding 3′-F-$dT(pT)_{15}$ is larger than that determined from either the 2-AP or Trp fluorescence experiments. If this difference is real, then this suggests the presence of yet another Rep monomer−ss DNA intermediate in Scheme 3. Furthermore, the estimate of k_1(app) obtained from Trp quenching is clearly an underestimate of the bimolecular rate constant since direct comparisons indicate that the intrinsic tryptophan fluorescence quenching lags behind the fluorescence enhancement of the 2-AP labeled DNA (see Figure 3A). Therefore, the signal associated with Trp quenching may reflect a fast conformational change occurring subsequent to DNA binding.

The sum of the first-order rate constants for the isomerization step, $(k_2 + k_{-2})$, obtained from global analysis of the 2-AP data ($k_2 + k_{-2} = 2.9 \pm 0.9$ s^{-1}) is similar to that estimated from the plateau value for $k_{obs,2}$ from the fluorescein experiments ($k_2 + k_{-2} = 3.8 \pm 0.6$ s^{-1}). However, these are lower than the estimate determined from tryptophan quenching with $d(T_5AT_4AT_5)$ ($k_2 + k_{-2} = 8.5 \pm 1.0$ s^{-1}). This latter estimate may reflect differences due to DNA base composition.

Similar values for k_3, the apparent bimolecular rate constant for Rep dimerization to form P2S, are obtained from experiments monitoring either the fluorescence of $d(T_5(2\text{-AP})T_4(2\text{-AP})T_5)$ or 3′-F-$dT(pT)_{15}$. Under conditions of excess Rep, values of $k_3 = (7.4 \pm 0.4) \times 10^5$ M^{-1} s^{-1} and $(3.3 \pm 0.2) \times 10^5$ M^{-1} s^{-1} are obtained by monitoring 25 nM $d(T_5(2\text{-AP})T_4(2\text{-AP})T_5)$ and 5 nM 3′-F-$dT(pT)_{15}$, respectively. Both fluorescent oligodeoxynucleotides show a change in fluorescence emission intensity upon the addition of an unligated Rep monomer, an enhancement in the case of $dT_5(2\text{-AP})T_4(2\text{-AP})T_5$ and a fluorescence quenching following the 3′-F-$dT(pT)_{15}$ fluorescence. Global analysis of the $d(T_5(2\text{-AP})T_4(2\text{-AP})T_5)$ binding data gave a similar bimolecular rate constant of $(4.5 \pm 0.3) \times 10^5$ M^{-1} s^{-1} for Rep dimerization.

Although a quenching of Rep Trp fluorescence also occurs upon Rep dimerization, we did not attempt a quantitative analysis of the dimerization kinetics using this probe due to its sensitivity to photobleaching, which occurs over the same time scale as dimerization. However, the Rep Trp fluorescence was useful to demonstrate the extreme negative cooperativity for ss DNA binding to the two sites of the Rep dimer. Figure 3A shows that a quenching of Rep Trp fluorescence accompanies Rep dimerization under conditions where the half-ligated P_2S dimer is formed (i.e., in the presence of excess Rep monomer). However, upon mixing Rep with a large excess of ss DNA, the monomer becomes transiently saturated with ss DNA resulting in a quenching of the Trp fluorescence which is followed by a small but significant fluorescence recovery (6% of the original quenching), the rate of which coincides with the rate of Rep dimerization (see Figure 4). This recovery of Trp fluorescence reflects a net release of DNA upon formation of a small amount of P_2S. The doubly-ligated Rep dimer, P_2S_2 is unstable relative to P_2S even under conditions of excess DNA due to the large negative cooperativity for DNA binding to the Rep dimer that exists under these solution conditions (5 mM $MgCl_2$, no nucleotide) (Wong & Lohman, 1992).

Mechanism of DNA Dissociation from P_2S. The dissociation kinetics of $d(T_5(2\text{-AP})T_4(2\text{-AP})T_5$ (S) from the half-ligated P_2S Rep dimer were performed in the presence of a nonfluorescent competitor ss DNA. These experiments

indicate that dissociation of S from P_2S is slow in the absence of competitor DNA (0.0032 ± 0.0001 s^{-1}) and occurs by a pathway in which dissociation of the dimer is rate limiting (k_{-3} in Schemes 3 and 5). Global analysis of the Rep−(d(T_5-(2-AP)T_4(2-AP)T_5) kinetic data using the same ss oligodeoxynucleotide confirms this conclusion and yields the same rate constant for dimer dissociation (0.0027 ± 0.0006 s^{-1}). Therefore, direct dissociation of ss DNA from P_2S must occur more slowly than this and we estimate an upper limit of $\sim 5 \times 10^{-5}$ s^{-1} for this rate constant. Interestingly, the observed rate constant for ss DNA dissociation from P_2S increases with increasing competitor DNA concentration, which provides direct evidence for transient formation of the P_2S_2 dimer, with the dissociation rate of S from P_2S_2 being faster than from P_2S. Furthermore, the apparent bimolecular rate constant, k_4, for ss DNA binding to the unligated subunit of P_2S is macroscopically slow, with a lower limit of $k_4 > 250$ M^{-1} s^{-1}. This apparent bimolecular rate constant is much slower than that measured for ss DNA binding to the Rep monomer [$(3-7) \times 10^7$ M^{-1} s^{-1}], and thus binding of the second ss DNA to P_2S must occur by a multistep process.

Comparison with Equilibrium Constants Determined by Nitrocellulose Filter Binding. Wong et al. (1992) and Wong and Lohman (1992) have previously measured equilibrium constants for Rep−ss oligodeoxynucleotide (dN(pN_{15}) binding and Rep dimerization using a nitrocellulose filter binding technique (Wong & Lohman, 1993) under the same conditions used in the kinetic experiments reported here [4.0 °C, 20 mM Tris-HCl, pH 7.5, 6 mM NaCl, 5 mM $MgCl_2$, 5 mM 2-mercaptoethanol, 10% (v/v) glycerol]. The equilibrium scheme used to analyze the nitrocellulose filter binding data (Scheme 1) did not include the PS* intermediate shown in Scheme 3 since this intermediate was only observed in the kinetics experiments reported here. Therefore, only two equilibrium constants, K_{1S} and L_{2S}, were required to describe the equilibrium formation of the half-ligated Rep dimer P_2S (Wong et al., 1992; Wong & Lohman, 1992). The relationships between K_{1S} and L_{2S} and the equilibrium constants determined from the stopped-flow studies reported here, K_1, K_2, and K_3, are given in eqs 6 and 7.

$$K_{1S} = K_1(1 + K_2) \quad (6)$$

$$L_{2S} = K_2K_3/(1 + K_2) \quad (7)$$

Due to the large value of $K_2 = 13 \pm 6$, L_{2S} is essentially equivalent to K_3 and the equilibrium dimerization constant, L_{2S}, determined by filter binding [$L_{2S} = 200 \pm 40$ μM^{-1} (Wong & Lohman, 1992)] agrees well with that reported here ($K_3 = 170 \pm 50$ μM^{-1}). Furthermore, the negative cooperativity between the two DNA binding sites on the Rep dimer determined from the filter binding experiments is also clearly evident in the kinetic experiments (e.g., see Figures 4 and 6A), although we cannot make an accurate determination of the equilibrium constant for binding S to P_2S. However, the nitrocellulose filter binding method underestimates the equilibrium constant for Rep monomer binding to ss DNA under these conditions [$K_{1S} = 2.1 \pm 0.3$ μM^{-1} (Wong & Lohman, 1992) vs $K_1(1 + K_2) = 320 \pm 40$ μM^{-1}]. As judged by the experiment described in Figure 9, the equilibrium constants determined from the kinetic rate constants reported here (K_1, K_2, and K_3) (Table 1) provide a better description of the equilibrium population distribution of Rep−DNA species. The underestimation of the equilibrium constant for Rep monomer binding to dN($pN)_{15}$ may reflect differences in filter retention efficiencies of the two singly ligated species, PS and PS*, or the fact that nitrocellulose filter binding is not a true equilibrium technique.

Advantages of the Fluorescence Stopped-Flow Technique for Kinetic Studies of Protein-Nucleic Acid Interactions. The fluorescence stopped-flow technique used in the experiments reported here offers several advantages over other methods used to study protein DNA binding kinetics. The main advantage is that the kinetics can be monitored continuously. An additional advantage for the studies reported here is that the kinetics, as monitored by the fluorescence of the modified DNA (both 2-AP and fluorescein), are sensitive not only to the initial binding event, but also to protein conformational changes and the Rep assembly state. Changes in Rep Trp fluorescence also can be used to monitor these kinetics. Some of these fluorescence probes, have sufficiently high quantum yields to enable experiments to be performed at nM DNA concentrations. In fact, we routinely perform experiments using 1 to 5 nM fluorescein labeled DNA [see Figure 4 and Bjornson et al. (1994)] and 25 nM d(T_5(2-AP)T_4(2-AP)T_5) (see Figure 3B). This sensitivity enabled us to perform experiments that are near pseudo first order in protein concentration, which simplifies the kinetic analysis. Of course, one must be careful to determine whether the presence of the fluorescence probe modifies the mechanism. This does not seem to be a problem in the experiments reported here, since the same kinetic mechanism for DNA binding and DNA-induced Rep dimerization and similar rate constants are obtained from the analysis of kinetic data monitoring fluorescence probes on both the protein and the DNA. This indicates that the fluorescent probes, 2-AP and fluorescein, may also be useful as probes for investigating the kinetics of other protein−nucleic acid interactions. In fact, the fluorescent base 2-aminopurine has been used as a probe for studying the kinetics of DNA unwinding by helicases (Raney et al., 1994) and the kinetics of DNA synthesis by DNA polymerases (Bloom et al., 1993, 1994).

Mechanistic Implications for Rep-Catalyzed DNA Unwinding. A minimal kinetic mechanism along with estimates of the kinetic rate constants for ss oligodeoxynucleotide binding to Rep monomers and dimers and Rep dimerization are needed to understand the mechanism of Rep-catalyzed DNA unwinding *in vitro*. In the absence of accessory proteins, initiation of Rep-catalyzed duplex DNA unwinding *in vitro* requires a 3′-ss DNA flanking the duplex DNA (Amaratunga & Lohman, 1993). This ss DNA provides a high-affinity site for Rep monomer binding to the ss−ds DNA junction, and ss DNA binding induces Rep to dimerize to the active form of the helicase (Chao & Lohman, 1991; Wong et al., 1992; Wong & Lohman, 1992; Amaratunga & Lohman, 1993; Bjornson et al., 1994). The kinetic studies reported here indicate that binding of the Rep monomer to ss DNA (dN($pN)_{15}$) to form the PS complex is relatively rapid, with k_1(app) = $(3-6) \times 10^7$ M^{-1} s^{-1} at 4 °C. However, ss DNA binding to the Rep monomer is a two-step reaction, with an isomerization step (PS → PS*) following ss DNA binding, which increases the affinity of Rep monomer for ss DNA. In Scheme 3, we have assumed that this isomerization step is required for Rep dimerization, although we have not proven that PS cannot dimerize as well. However, a conformational change in the Rep monomer that favors dimerization is supported by the observation that Rep dimers are not detected in the absence of DNA even at total

Rep concentrations in excess of 10 μM (monomer) (Chao & Lohman, 1991; I. Wong, unpublished experiments).

Single-turnover kinetic studies by Bjornson et al. (1994), performed by pre-incubating short 18−24 bp duplexes possessing a 3′-ss DNA tail (dT_{20}) with excess Rep protein, indicate that Rep-catalyzed DNA unwinding occurs in two phases. A rapid phase, occurring with a rate constant of 1.3 ± 0.2 s^{-1} (25 °C), is independent of [Rep] reflecting unwinding of preformed productive Rep−DNA complexes. However, this is followed by a slower unwinding phase with an observed rate constant that increases linearly with increasing [Rep], reflecting an apparent bimolecular rate constant of $\sim(1.8 \pm 0.1) \times 10^5$ M^{-1} s^{-1} (25 °C). At 4 °C, we measure a rate constant for Rep dimerization ($P + PS^* \rightarrow P_2S$) of $(4.5 \pm 0.3) \times 10^5$ M^{-1} s^{-1}, which suggests that Rep dimerization is at least partially rate-limiting for the slower phase of DNA unwinding.

The kinetics experiments reported here also indicate that the rate of dissociation of ss DNA from the P_2S Rep dimer is quite slow, consistent with its high affinity ($\geq 5 \times 10^{13}$ M^{-1} under these conditions). In fact, dissociation of S from P_2S does not seem to occur directly, and rather the preferred pathway is via dissociation of the P_2S dimer to form $P + PS^*$ ($k_{-3} = 0.0027 \pm 0.0008$ s^{-1}) followed by rapid dissociation of ss DNA from PS*. Such slow dissociation of the Rep dimer from ss DNA is a requirement for processive unwinding by a helicase. However, we also show that ss DNA binding to the second subunit of the Rep dimer increases the net rate of dissociation of ss DNA. This influence of DNA binding to the second site of the Rep dimer on the rate of dissociation of DNA from the first site is likely to be important for the mechanism of DNA unwinding and translocation of the Rep dimer along ss DNA as suggested previously (Wong & Lohman, 1992). It remains to be determined how ATP binding and subsequent hydrolysis influence these rate constants since this will be important for understanding the mechanism of Rep-catalyzed DNA unwinding and Rep translocation.

ACKNOWLEDGMENT

We thank Isaac Wong for the observation that Rep Trp fluorescence is quenched upon binding ss DNA and for his help in analysis of these studies and Bill van Zante for his excellent technical assistance in the synthesis and purification of the oligodeoxynucleotides used in this study. We also thank Isaac Wong for discussions and a critical reading of the manuscript.

REFERENCES

Amaratunga, M., & Lohman, T. M (1993) *Biochemistry 32*, 6815−6820.
Arai, N., & Kornberg, A. (1981) *J. Biol. Chem. 256*, 5294−5298.
Arai, N., Arai, K. I., & Kornberg, A. (1981) *J. Biol. Chem. 256*, 5287−5293.
Barshop, B. A., Wrenn, R. F., & Frieden, C. (1983) *Anal. Biochem. 130*, 134−145.
Bjornson, K. P., Amaratunga, M., Moore, K. J. M., & Lohman, T. M. (1994) *Biochemistry 33*, 14306−14316.
Bloom, L. B., Otto, M. R., Beechem, J. M., & Goodman, M. F. (1993) *Biochemistry 32*, 11247−11258.
Bloom, L. B., Otto, M. R., Eritja, R., Reha-Krantz, L. J., Goodman, M. F., & Beechem, J. M. (1994) *Biochemistry 33*, 7576−7586.
Bridges, B. A., & von Wright, A. (1981) *Mutat. Res. 82*, 229−238.
Calendar, R., Lindqvist, B., Sironi, G., & Clark, A. J. (1970) *Virology 40*, 72−83.
Chao, K., & Lohman, T. M. (1991) *J. Mol. Biol. 221*, 1165−1181.
Colasanti, J., & Denhardt, D. T. (1987) *Mol. Gen. Genet. 209*, 382−390.
Daniels, D. L., Plunkett, G., Burland, V., & Blattner, F. R. (1992) *Science 257*, 771−778.
Denhardt, D. T., Dressler, D. H., & Hathaway, H. (1967) *Proc. Natl. Acad. Sci. U.S.A. 57*, 813−820.
Guest, C. R., Hochstrasser, R. A., Sowers, L. C., & Millar, D. P. (1991) *Biochemistry 30*, 3271−3279.
Hanawalt, P. C. (1994) *Science 266*, 1957−1958.
Johnson, K. A. (1992) in *The Enzymes*, Vol. 20, pp 1−61, Academic Press, Inc., New York.
Kornberg, A., Scott, J. F., & Bertsch, L. L. (1978) *J. Biol. Chem. 253*, 3298−3304.
Lane, H. E. D., & Denhardt, D. T. (1974) *J. Bacteriol. 120*, 805−814.
Lane, H. E. D., & Denhardt, D. T. (1975) *J. Mol. Biol. 97*, 99−112.
Lohman, T. M. (1992) *Mol. Microbiol. 6*, 5−14.
Lohman, T. M. (1993) *J. Biol. Chem. 268*, 2269−2272.
Lohman, T. M., & Bjornson, K. P. (1996) *Annu. Rev. Biochem. 65*, 169−214.
Lohman, T. M., Chao, K., Green, J. M., Sage, S., & Runyon, G. (1989) *J. Biol. Chem. 264*, 10139−10147.
Matson, S. W., & Kaiser-Rogers, K. A. (1990) *Annu. Rev. Biochem. 59*, 289−329.
Matson, S. W., Bean, D. W., & George, J. W. (1994) *BioEssays 16*, 13−22.
Moore, K. J. M., & Lohman, T. M. (1994a) *Biochemistry 33*, 14550−14564.
Moore, K. J. M., & Lohman, T. M. (1994b) *Biochemistry 33*, 14565−14578.
Moore, K. J. M., & Lohman, T. M. (1995) *Biophys. J. 68*, 180s−185s.
Nordlund, T. M., Xu, D., & Evans, K. O. (1993) *Biochemistry 32*, 12090−12095.
Patel, S. S., Wong, I., & Johnson, K. A. (1991) *Biochemistry 30*, 515−526.
Raney, K. D., Sowers, L. C., Millar, D. P., & Benkovic, S. J. (1994) *Proc. Natl. Acad. Sci. U.S.A. 91*, 6644−6648.
Scott, J. F., Eisenberg, S., Bertsch, L. L., & Kornberg, A. (1977) *Proc. Natl. Acad. Sci. U.S.A. 74*, 193−197.
Ward, D. C., Reich, E., & Stryer, L. (1969) *J. Biol. Chem. 244*, 1228−1237.
Wong, I., & Lohman, T. M. (1992) *Science 256*, 350−355.
Wong, I., & Lohman, T. M. (1993) *Proc. Natl. Acad. Sci. U.S.A. 90*, 5428−5432.
Wong, I., Moore, K. J. M., Bjornson, K. P., Hsieh, J., & Lohman, T. M. *Biochemistry* (submitted).
Wong, I., Chao, K. L., Bujalowski, W., & Lohman, T. M. (1992) *J. Biol. Chem. 267*, 7596−7610.
Wong, I., Amaratunga, M., & Lohman, T. M. (1993) *J. Biol. Chem. 268*, 20386−20391.
Yarranton, G. T., & Gefter, M. L. (1979) *Proc. Natl. Acad. Sci. U.S.A. 76*, 1658−1662.
Zimmerle, C. T., & Frieden, C. (1989) *Biochem. J. 258*, 381−387.

BI9522763